Workshop, Géométrie et matériaux, 13/05/2019

NANOPARTICLES AND SELF-ASSEMBLY

Simon Tricard

Laboratoire de Physique et Chimie des Nano-Objets, Equipe Nano-structures et Chimie Organométallique,
INSA, CNRS, Université de Toulouse

Nanoobjects

Self-assembly of nanoobjects

Binary assemblies

Molecule oriented supraparticular chemistry

Nanoobjects

Self-assembly of nanoobjects

Binary assemblies

Molecule oriented supraparticular chemistry

NANOOBJECTS

NANOPARTICLE

A nanoobject the three dimension of which are at the nanometric scale,
i.e. a particle spanning 1–100 nm in diameter.

ISO TS/27687

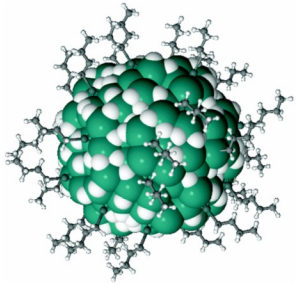

(QUANTUM) CONFINEMENT

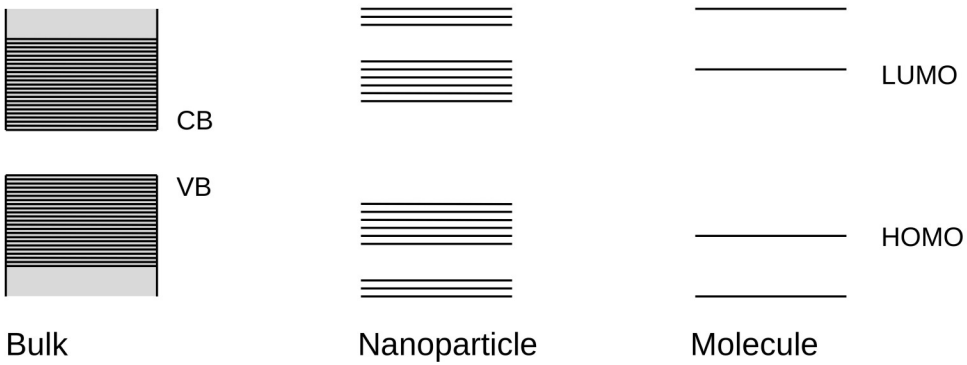

Quantum dots

SURFACE EFFECTS

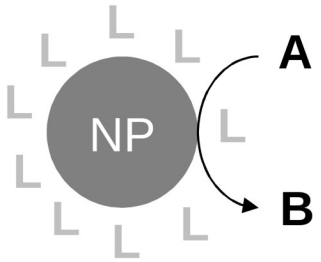

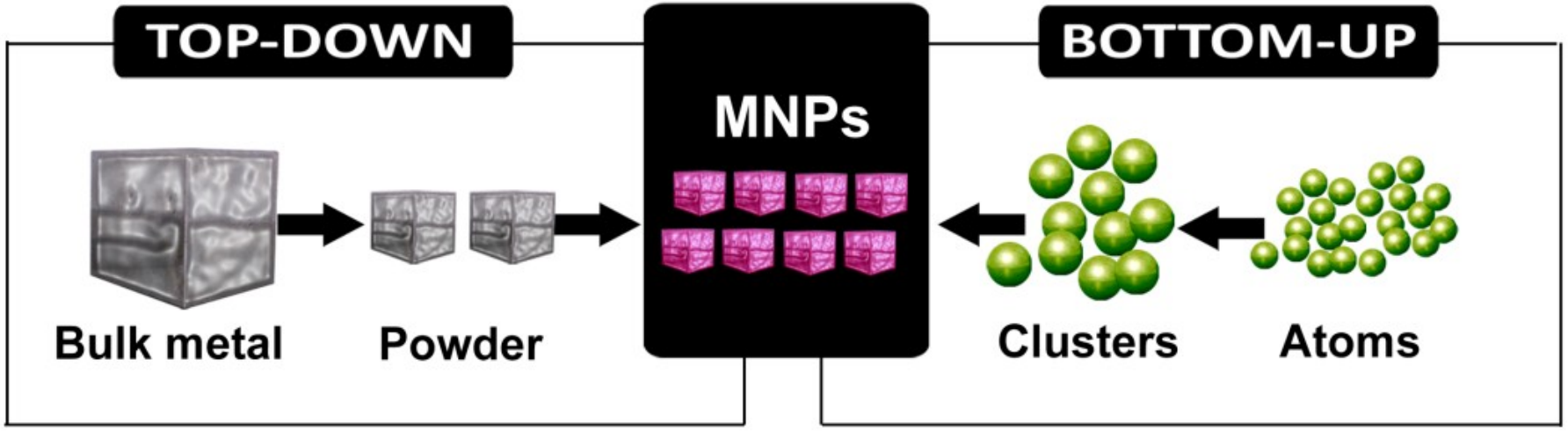
TOP-DOWN
BOTTOM-UP
MNPs
Bulk metal
Powder
Clusters
Atoms

Synthèse Organométallique de Nanoparticules

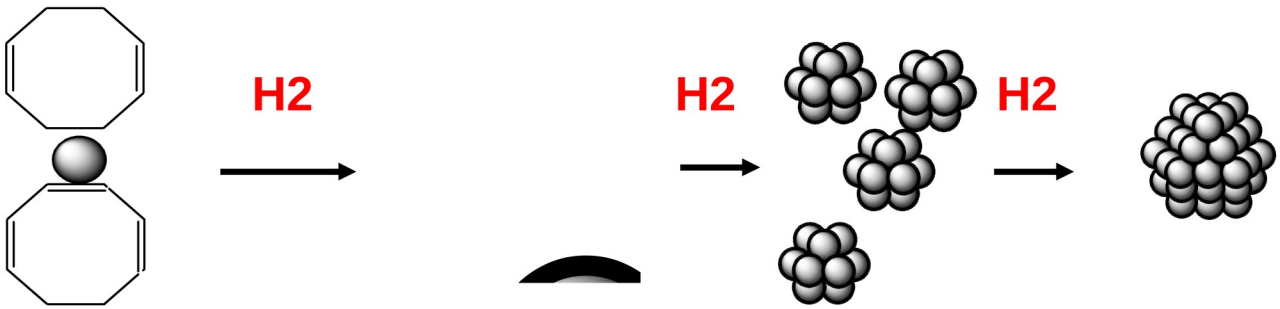

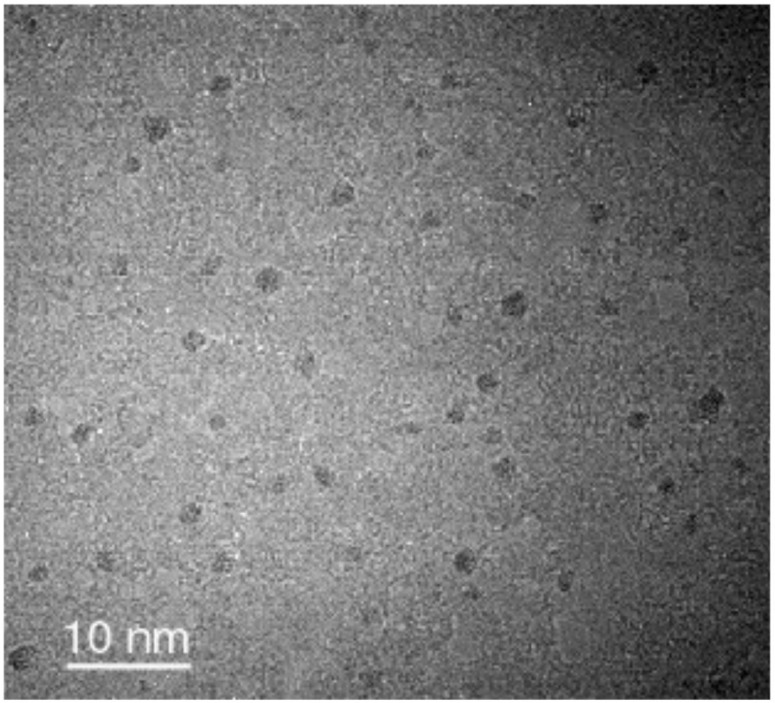

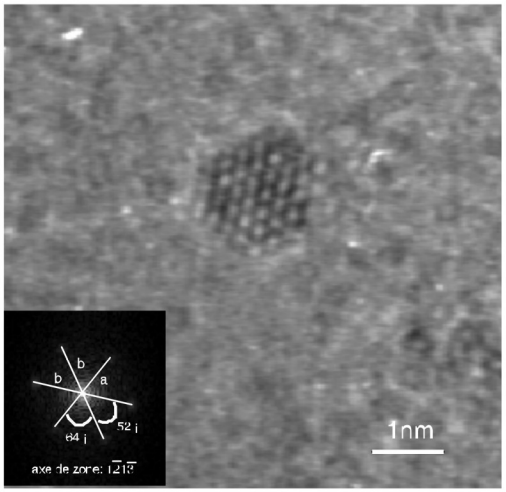

Problématique : maîtrise de la croissance, contrôle de l'état de surface, de la taille, de la forme et de l'organisation des nanoparticules.

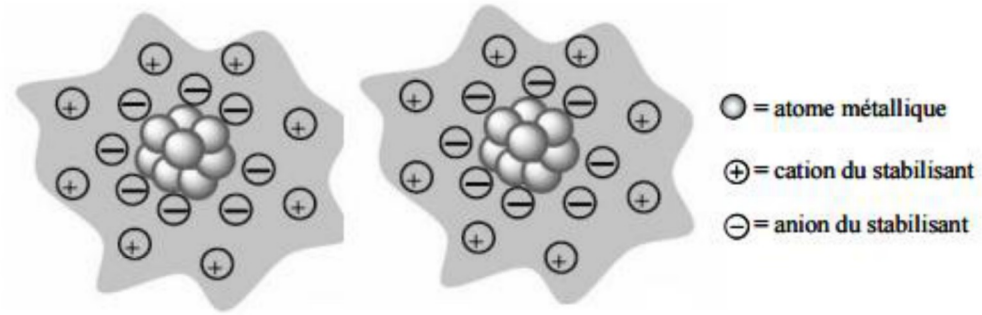
= atome métallique
= cation du stabilisant
= anion du stabilisant

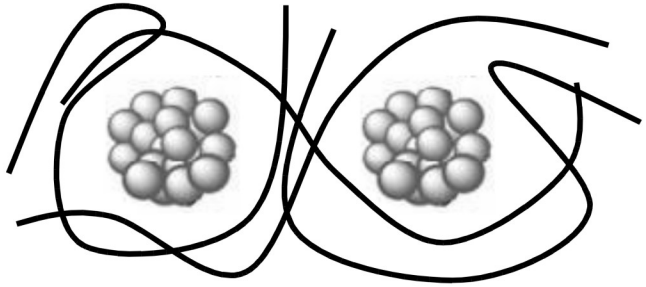

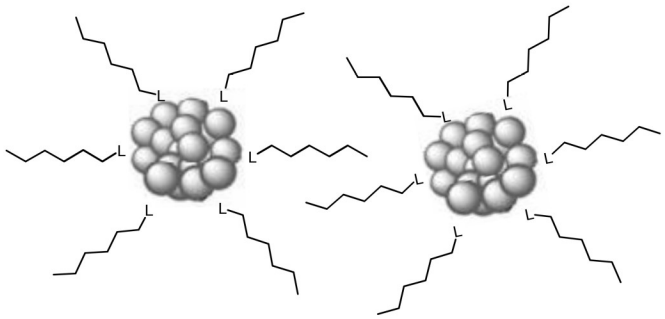

Plasmonics

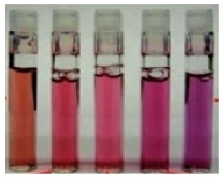

(a) (b) (c) (d) (e)

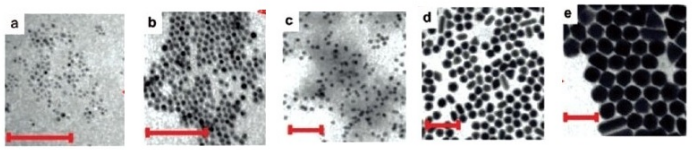

Effect of particle size on gold nanoparticle dispersion color

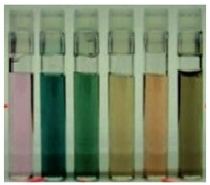

(f) (g) (h) (i) (j) (k)

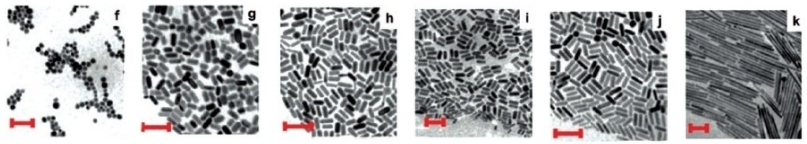

Effect of aspect ratio on gold nanoparticle dispersion color

Hyperthermia

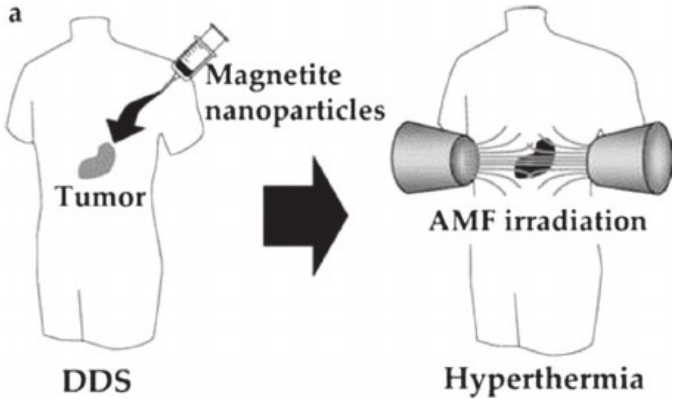

Electronics

Coulomb Blockade in a Quantum Dot Circuit -13

Experimental results showing the Coulomb staircase are shown in the figure. In this experiment, the setup consisted of an In droplet separated from an Al ground plane by a tunneling oxide layer approximately 1 nm thick. An STM tip is brought into close proximity to the droplet, forming a metal-insulator-island-insulator-metal junction, as depicted in the figure below.

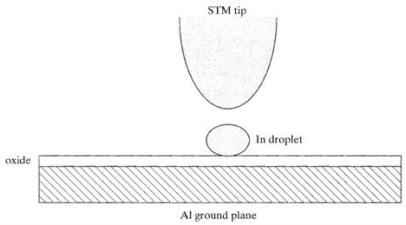

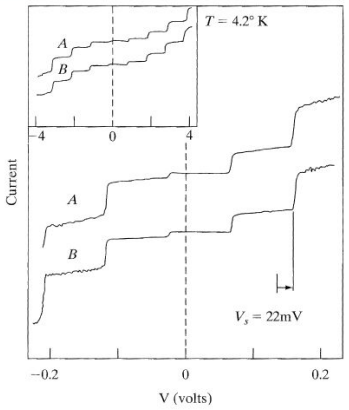

From Wilkins, R., E. Ben-Jacob, and R. C. Jaklevic, "Scanning-Tunneling-Microscope Observations of Coulomb Blockade and Oxide Polarization in Small Metal Droplets," Phys. Rev. Lett. 63 (1989)

Catalysis

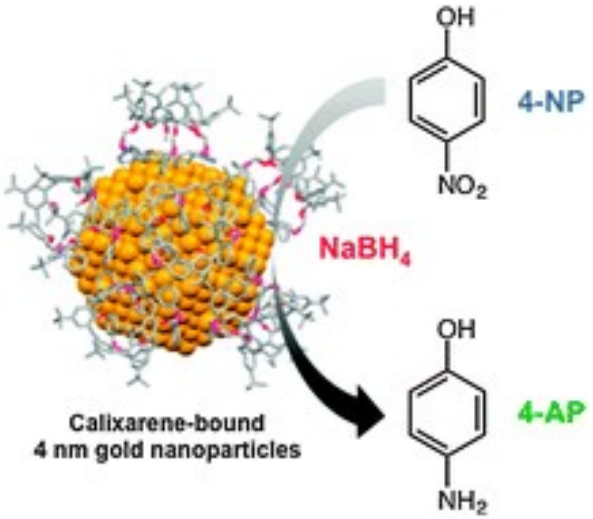

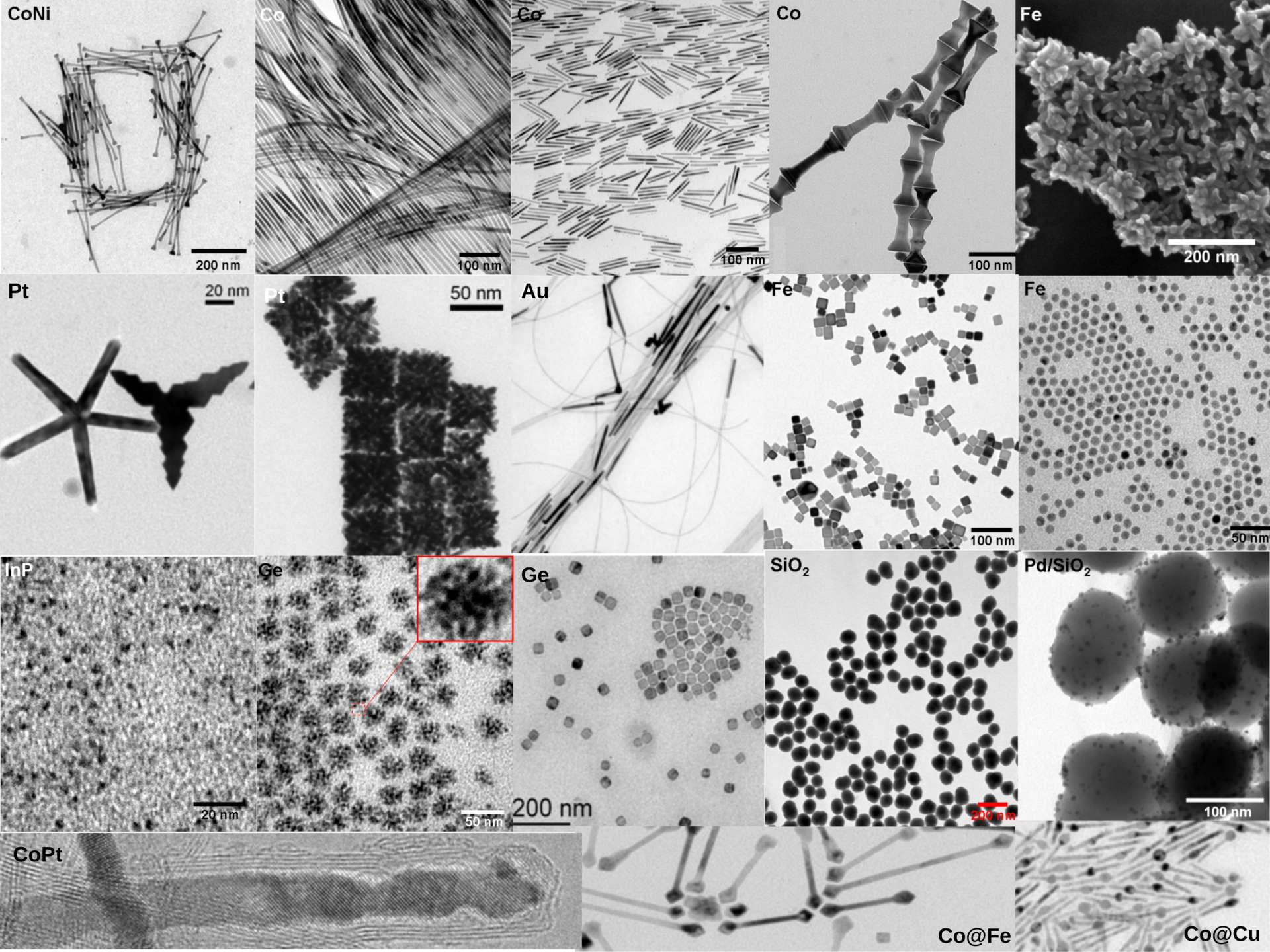
CoNi
200 nm
Co
100 nm
Co
100 nm
Co
100 nm
Fe
200 nm
Pt
20 nm
Pt
50 nm
Au
Fe
100 nm
Fe
50 nm
InP
20 nm
Ge
50 nm
Ge
200 nm
SiO2
200 nm
Pd/SiO2
100 nm
CoPt
Co@Fe
Co@Cu

Nanoobjects

Self-assembly of nanoobjects

Binary assemblies

Molecule oriented supraparticular chemistry

NANOPARTICLE SELF-ASSEMBLY

SUPERCRISTALS

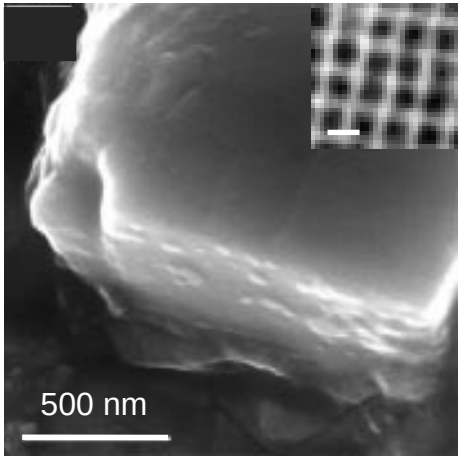

Chaudret, et al. 2004

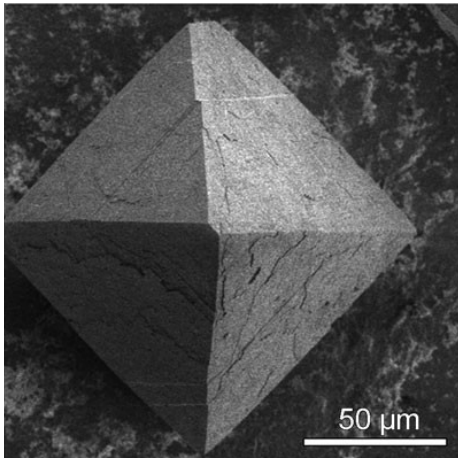

Eychmüller, et al. 2012

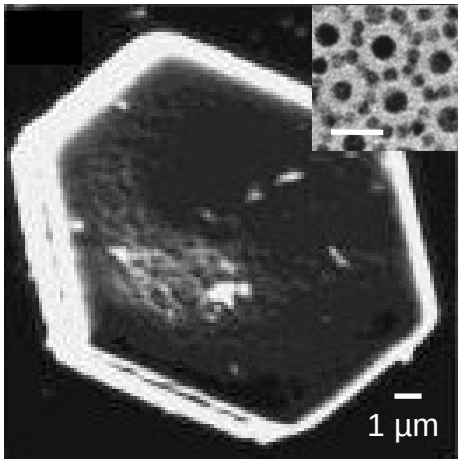

Murray, et al. 2006

3D ordered Superlattices (SLs) of Ag or Au NPs

TEM and SEM

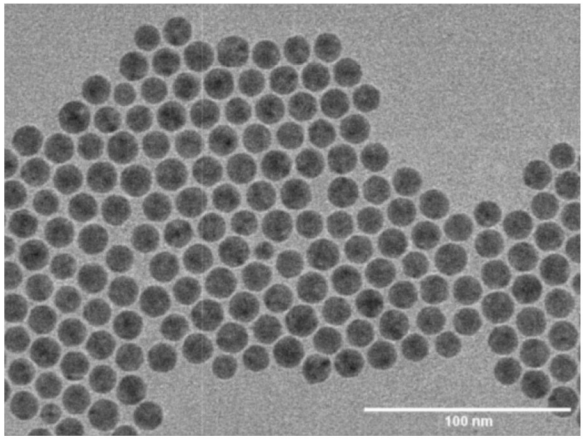

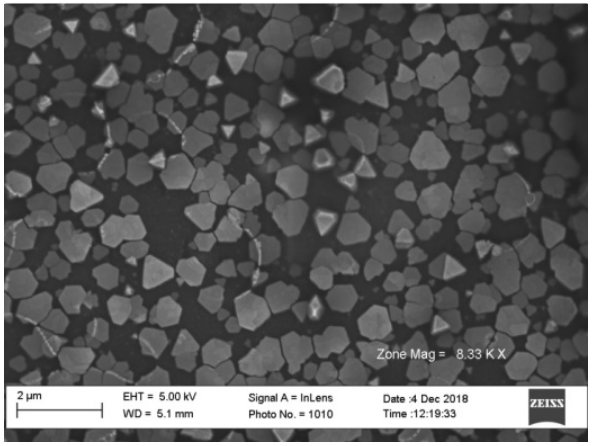

Effect of NP crystallinity

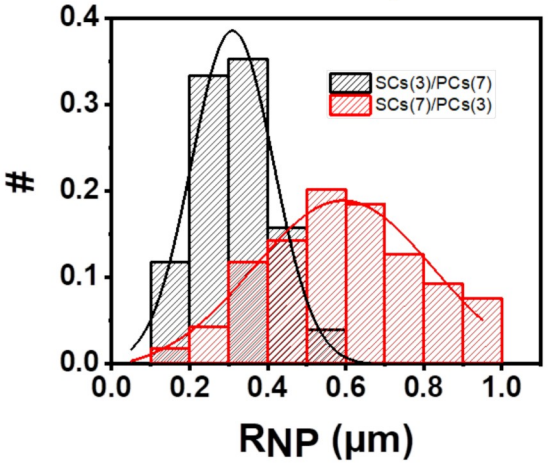

3D Self-assembly

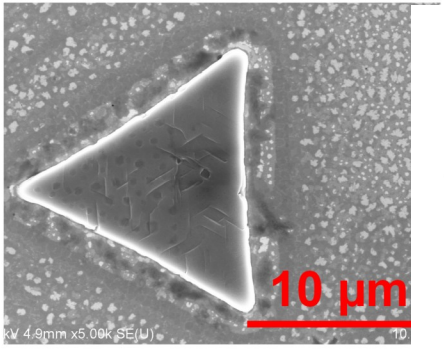

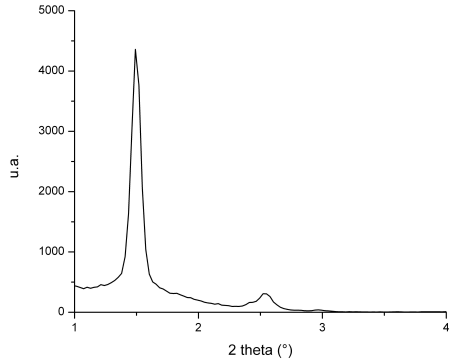

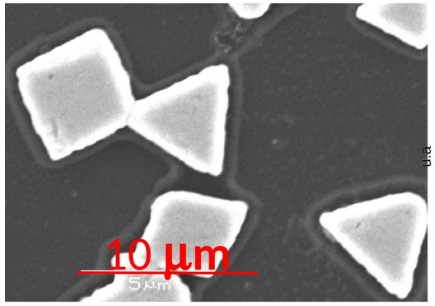

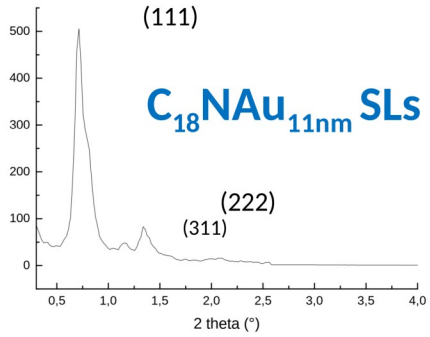

A.Courty et al, Chem Mater 2016, *28, 4380-4389*/Chem.Phys.chem, 2017 DOI: 10.1002/cphc.201700601

PhD Thesis of Suyeon Lee, laboratoire MONARIS, Paris France

Thanks to Alexa Courty

Réseaux NPs Sn : position+orientation cristallographique

Réseaux NPs In : position

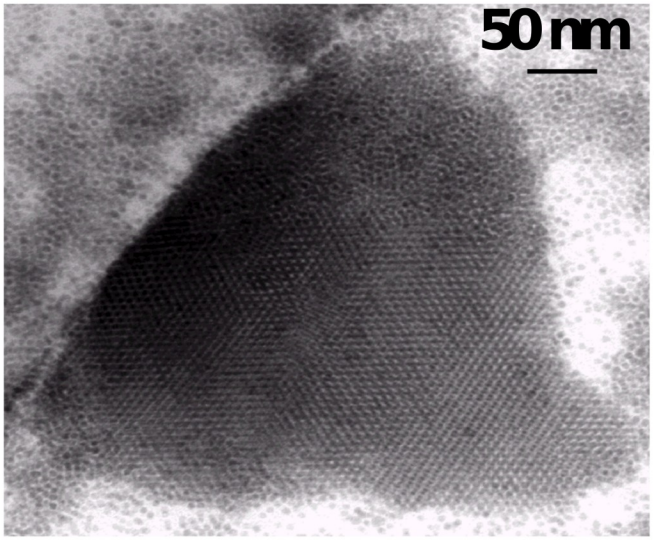

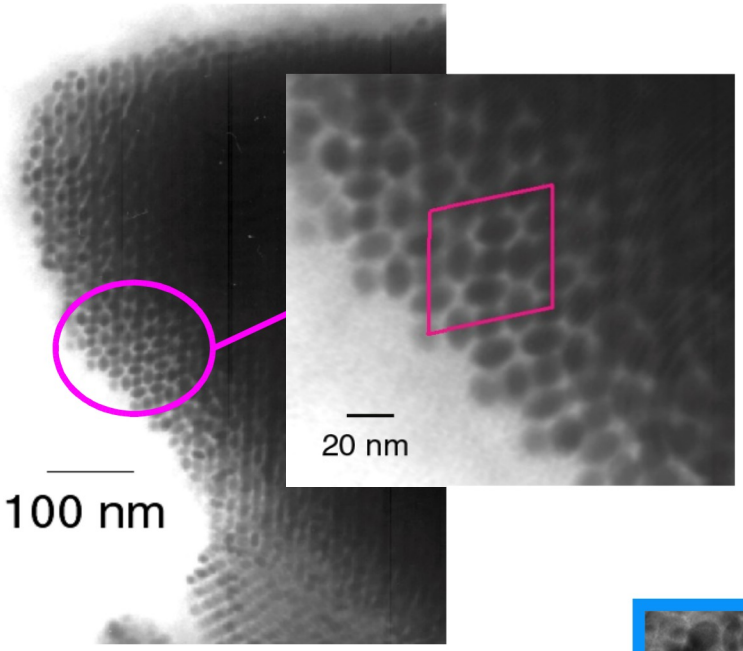

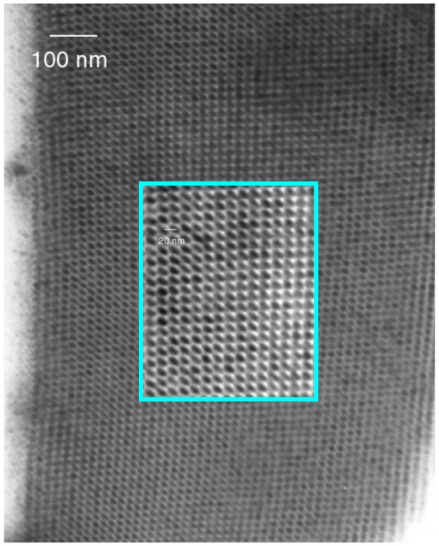

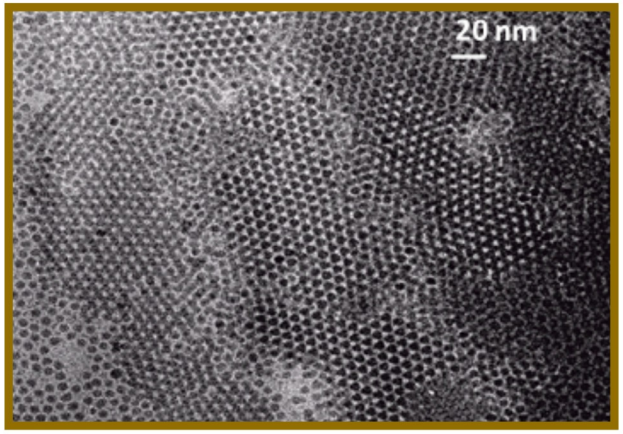

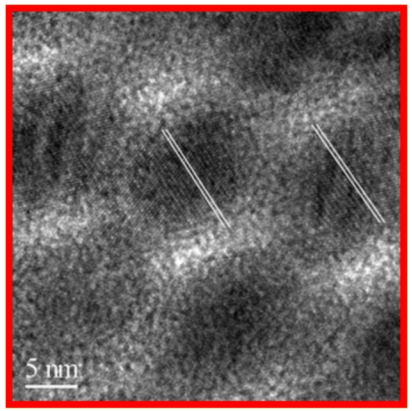

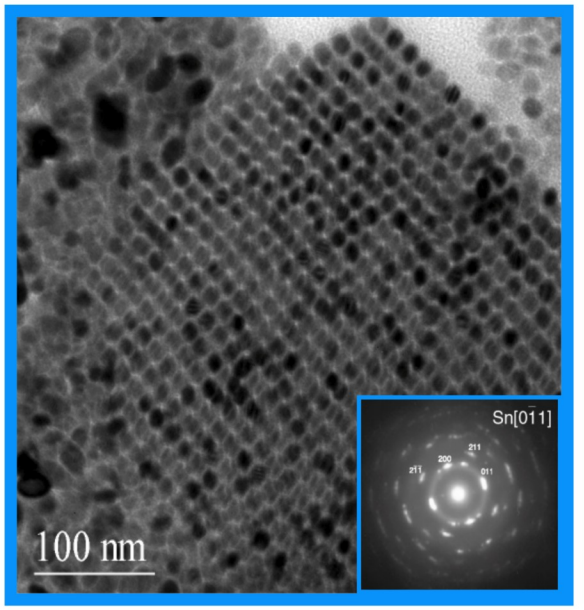

Angew. Chem. Int. Ed. ***2001***, *40, 448*

Angew. Chem. Int. Ed. ***2003***, *42, 1945*

Thanks to Katerina Soulantika

Fast destabilization with an anti-solvent

Square

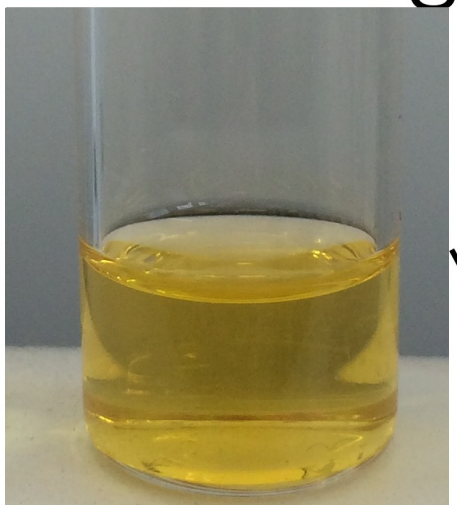

ethanol

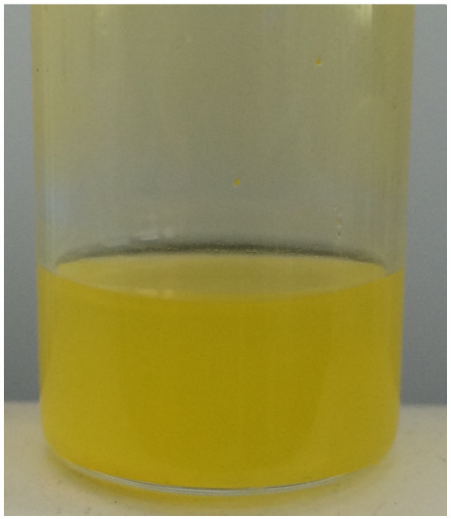

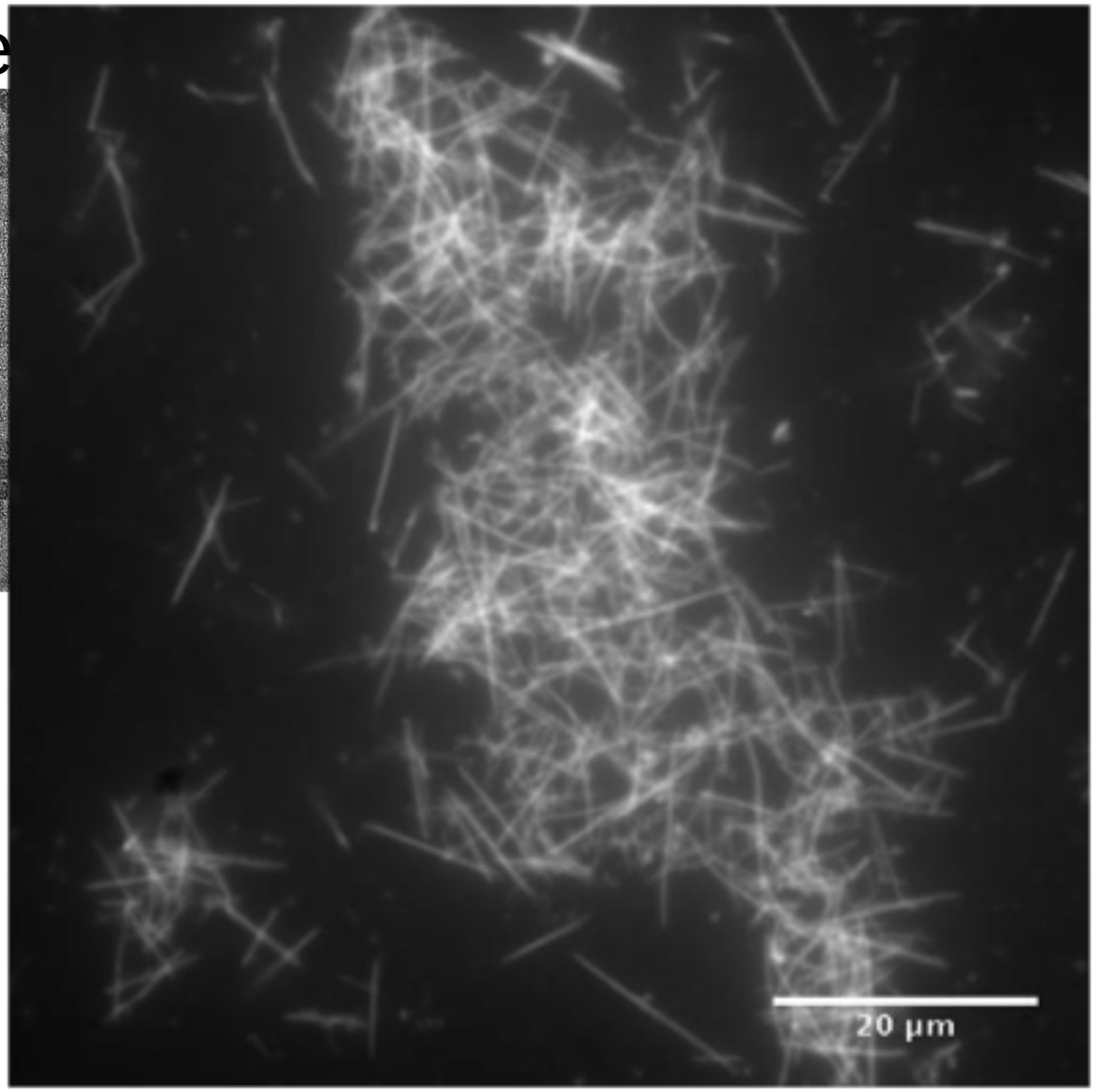

Anisotropic particles (~5-15 µm)

Thanks to Benjamin Abecassis

Structure of the needles: TEM

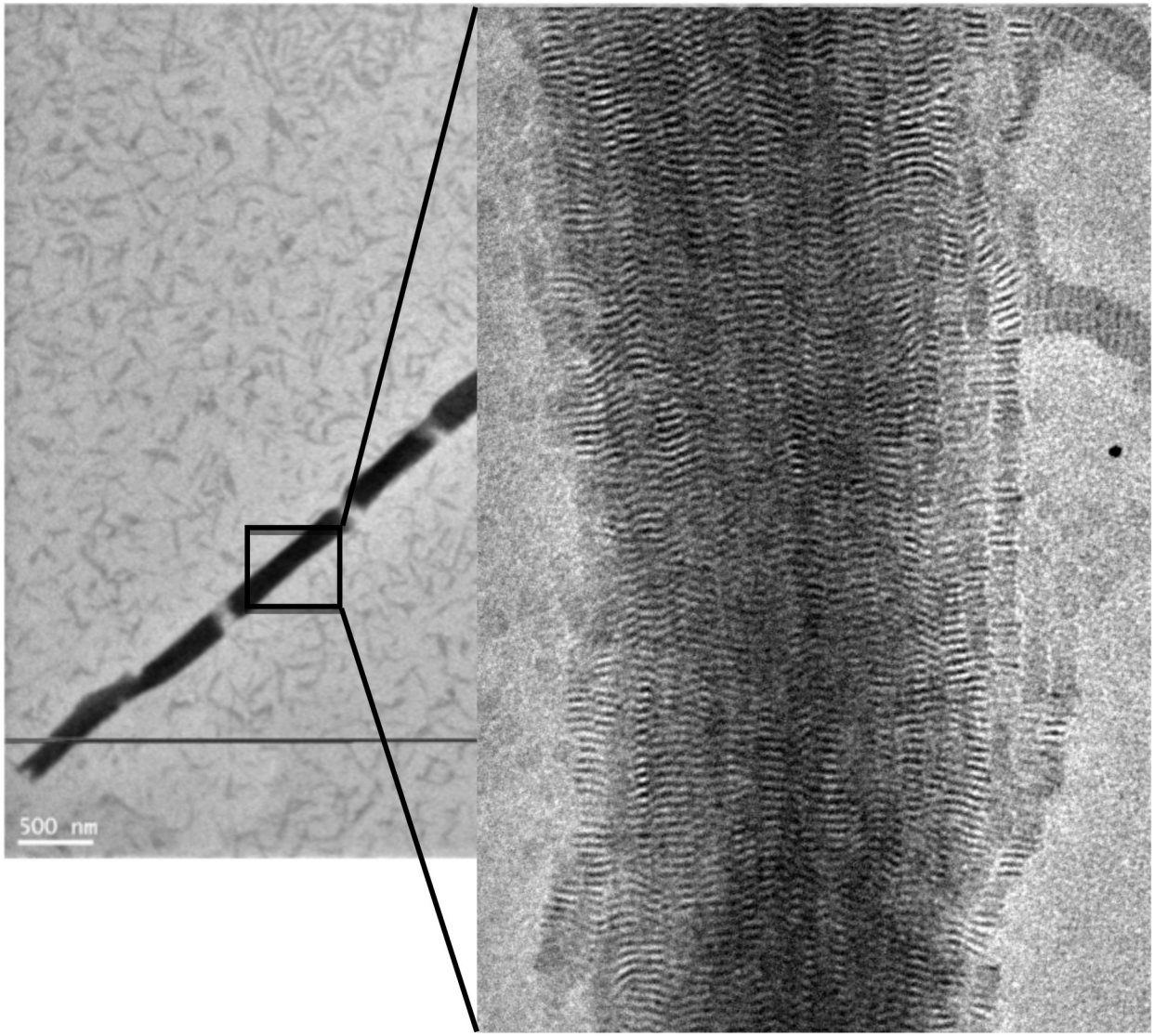

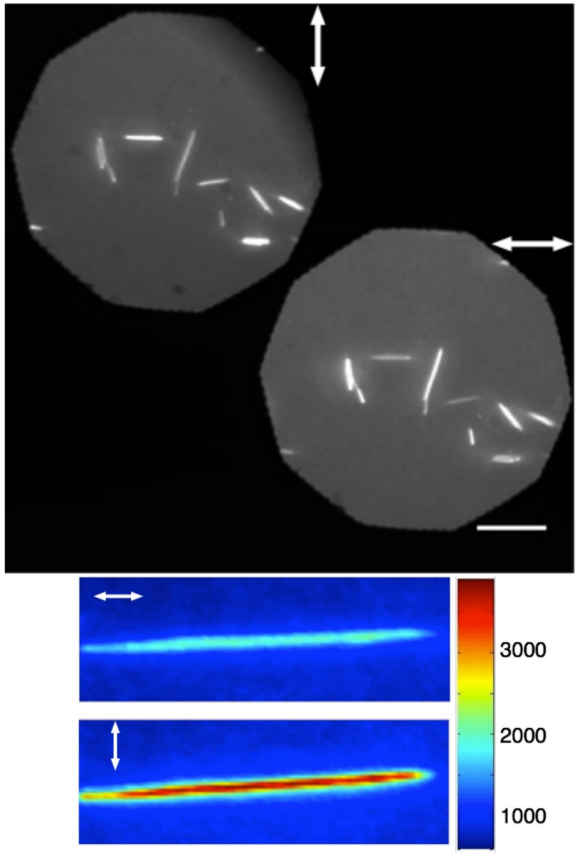

Giant microneedles composed of 10^6 nanoparticles

Abécassis et al, Nano Lett, 2014

Thanks to Benjamin Abecassis

Self-assembly through slow drying

Oleic acid

Colloidal dispersion of NPL in hexane

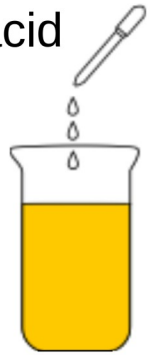

Slow drying

3 days

redispersion

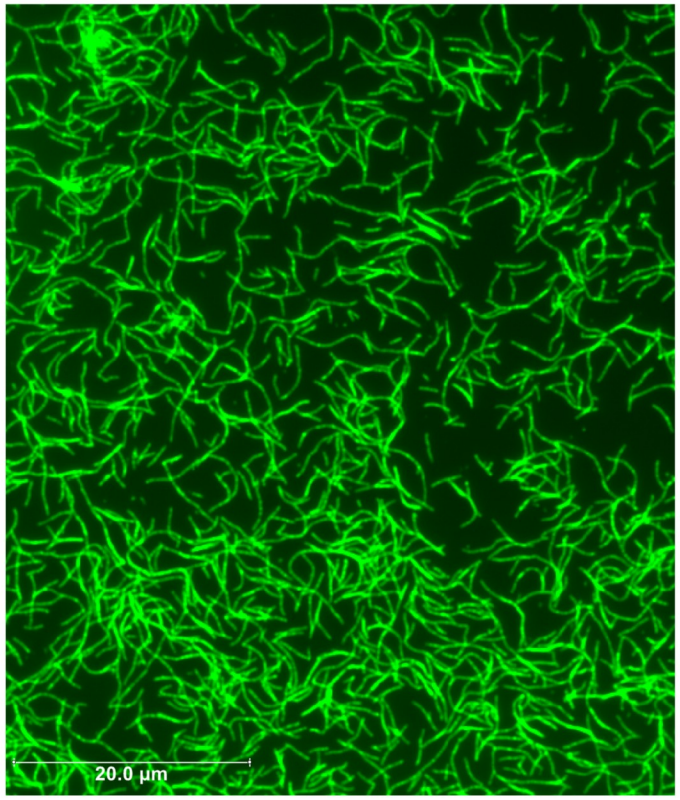

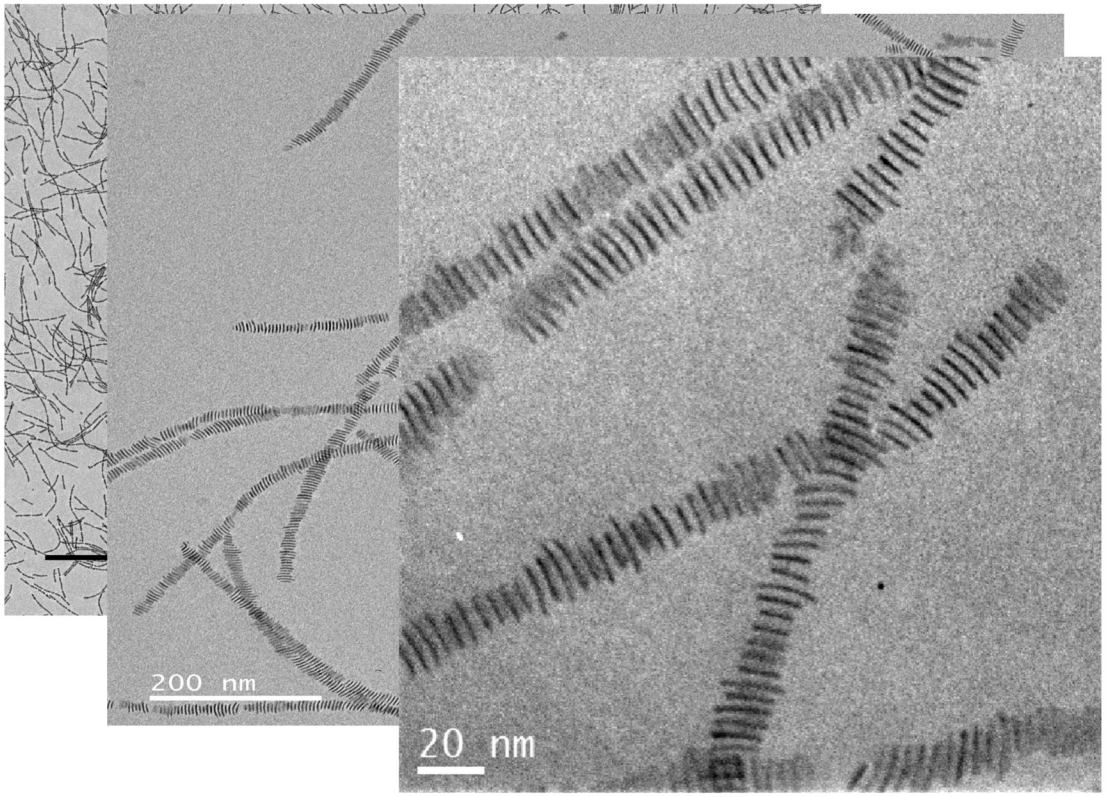

Thanks to Benjamin Abecassis

Etude in situ XAS – SAXS (X-ray Absorption Spectroscopy – Small Angle X-ray Scattering)

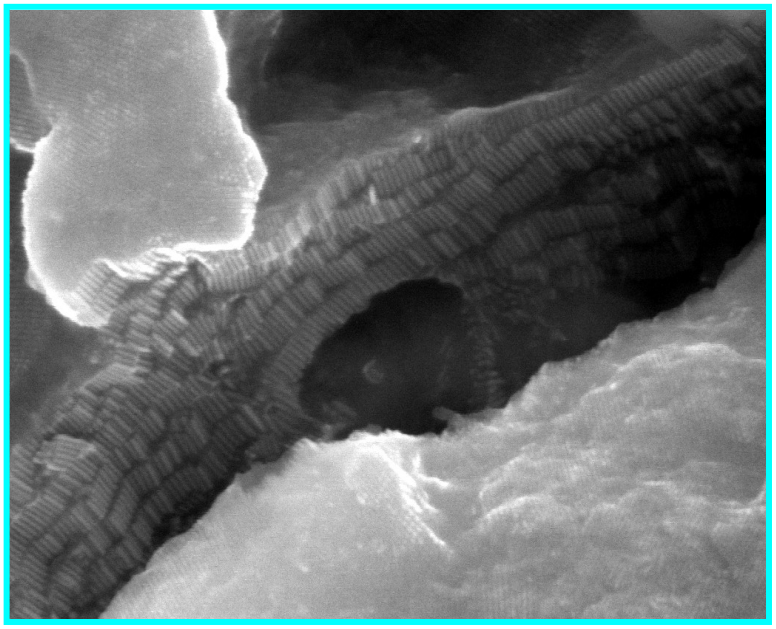

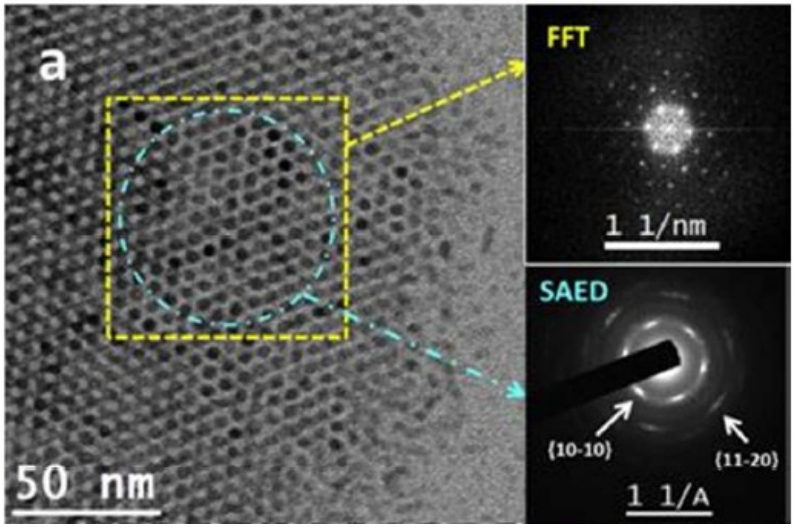

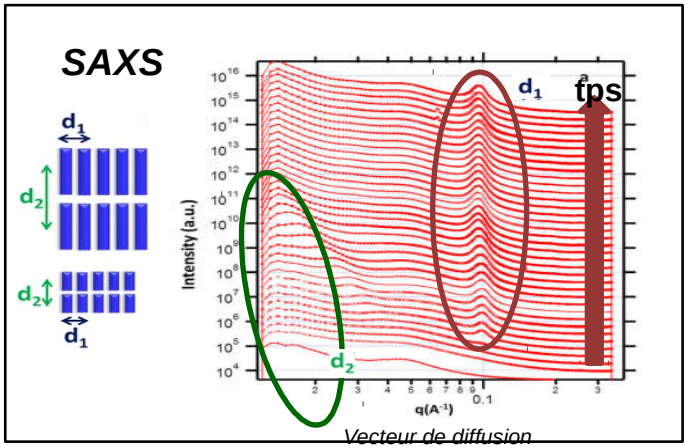

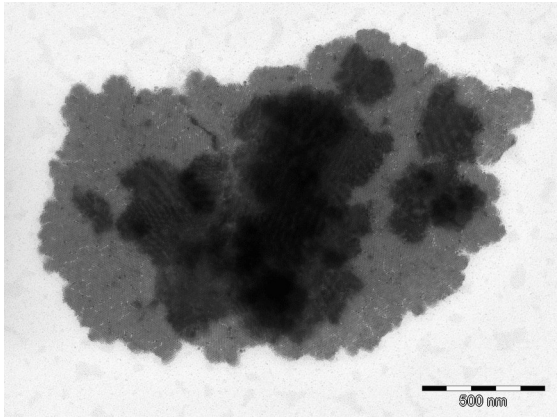

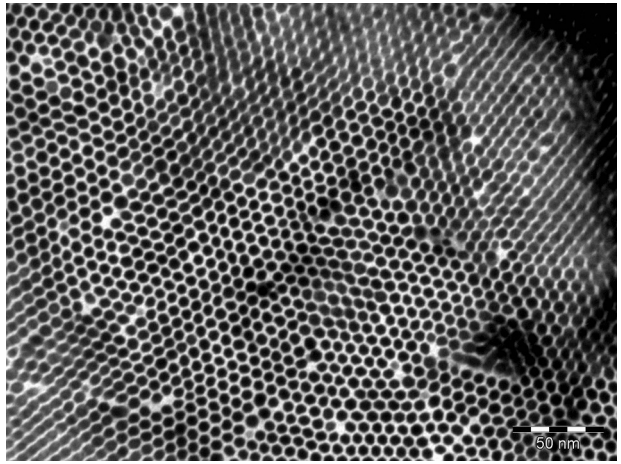

***J. Am. Chem. Soc.*, 2016, 8422**

Thanks to Katerina Soulantika

JACS
JOURNAL OF THE AMERICAN CHEMICAL SOCIETY
Article
pubs.acs.org/JACS

Formation of Diverse Supercrystals from Self-Assembly of a Variety of Polyhedral Gold Nanocrystals

Ching-Wen Liao,[†] Yeh-Sheng Lin,[†] Kaushik Chanda,[†] Yen-Fang Song,[‡] and Michael H. Huang*[,†]

[†]Department of Chemistry, National Tsing Hua University, Hsinchu 30013, Taiwan
[‡]National Synchrotron Radiation Research Center, Hsinchu 30076, Taiwan

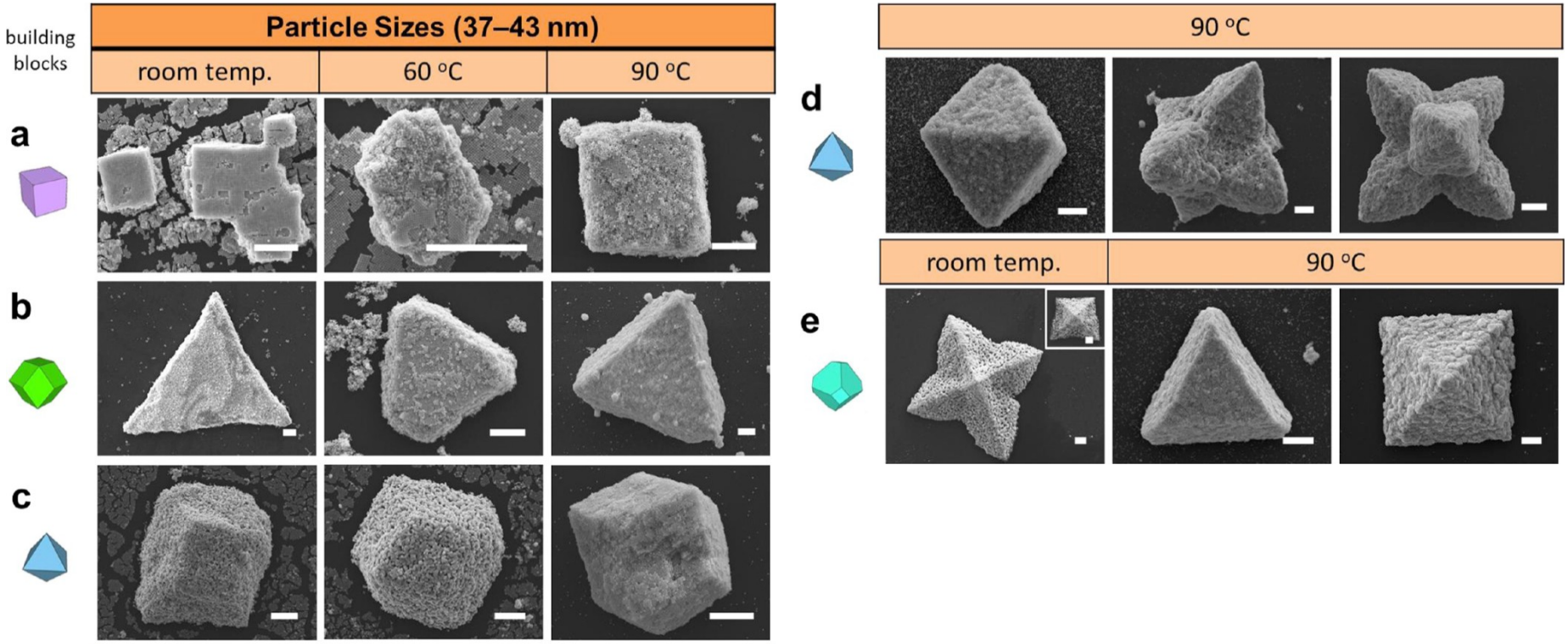

DOI: 10.1021/jacs.5b09959
J. Am. Chem. Soc. 2015, 137, 14773−14784

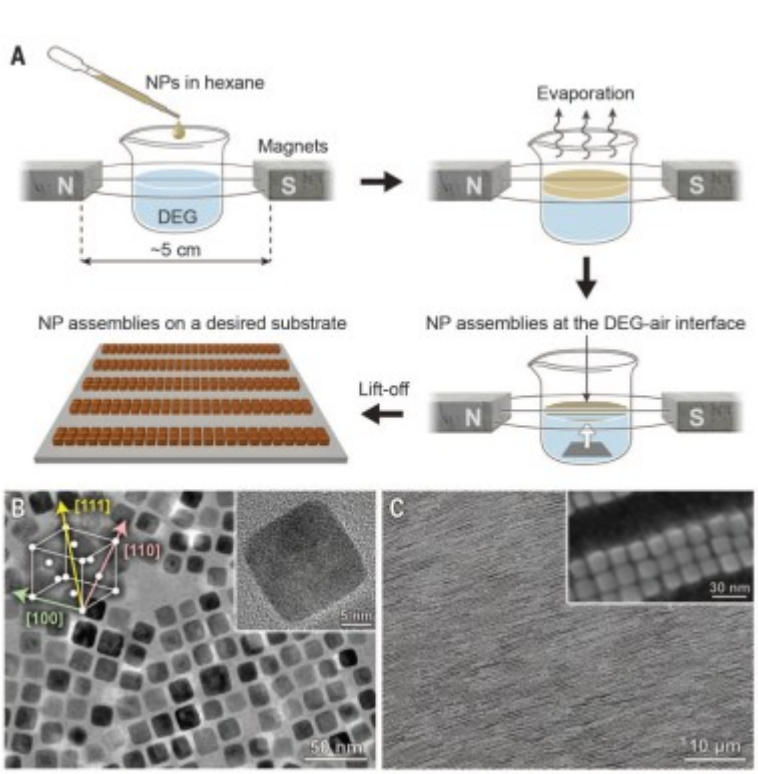

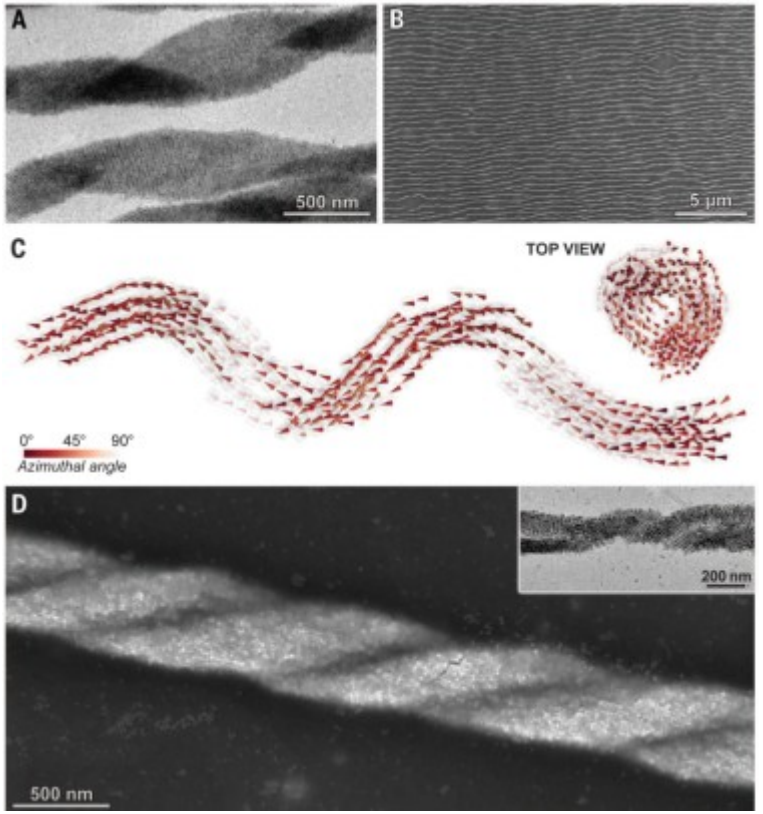

Singh, Gurvinder, Henry Chan, Artem Baskin, Elijah Gelman, Nikita Repnin, Petr Král, et Rafal Klajn. « Self-Assembly of Magnetite Nanocubes into Helical Superstructures ». *Science* 345, nº 6201 (5 septembre 2014): 1149-53. https://doi.org/10.1126/science.1254132.

Complex nano-object

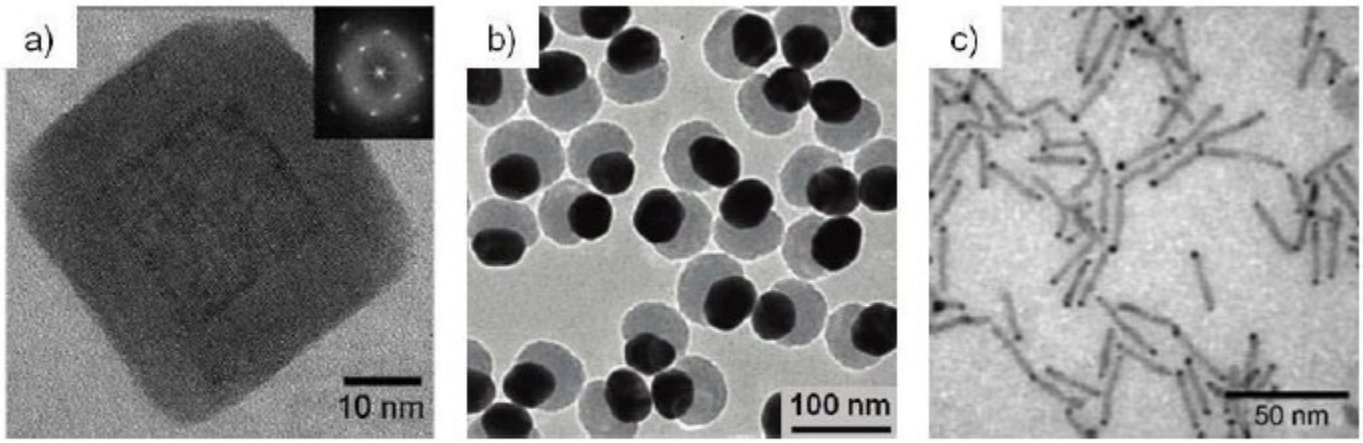

Figure 2 : Exemples de nano-objets complexes : a) nano-particules cœur-coquille d'analogues de bleu de Prusse CsFeCr@CoCr – encart : motif de diffraction ; b) nano-objets Janus d'Au-SiO_2 ; c) nano-haltères d'Au@CdSe.

Nanoobjects

Self-assembly of nanoobjects

Binary assemblies

Molecule oriented supraparticular chemistry

Assembly

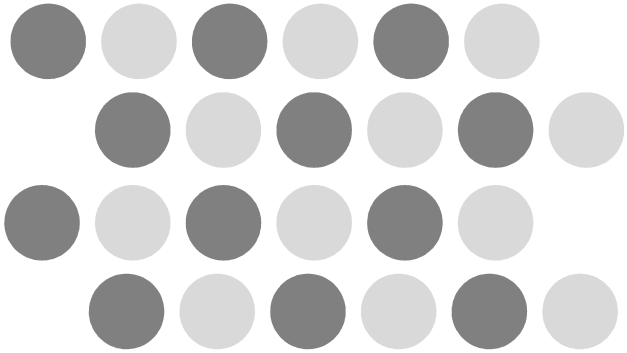

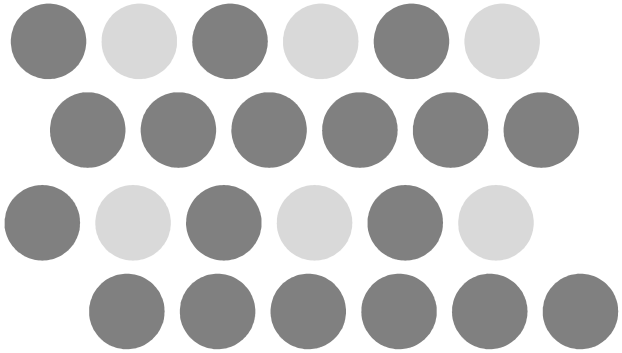

Electrostatic Self-Assembly of Binary Nanoparticle Crystals with a Diamond-Like Lattice

21 APRIL 2006 VOL 312 SCIENCE www.sciencemag.org

Alexander M. Kalsin, Marcin Fialkowski, Maciej Paszewski, Stoyan K. Smoukov, Kyle J. M. Bishop, Bartosz A. Grzybowski*

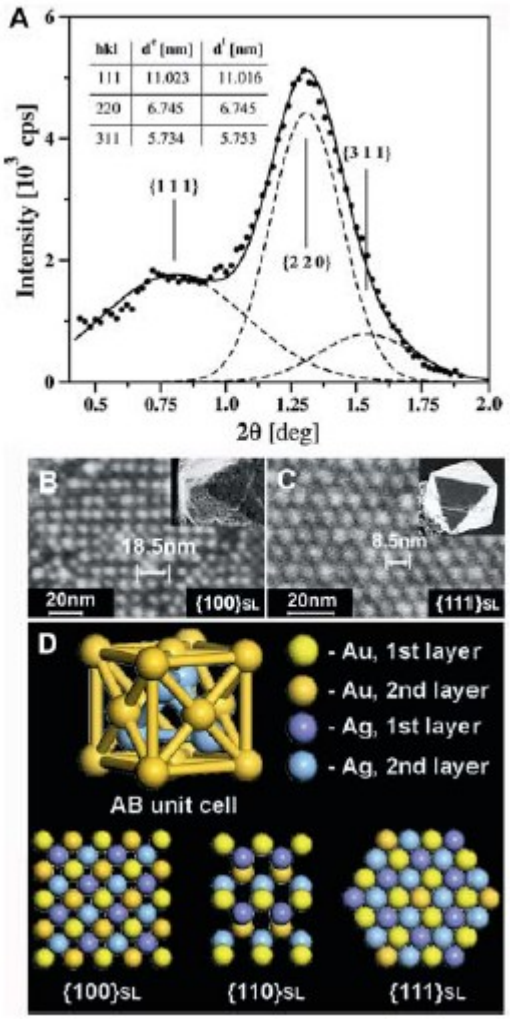

Fig. 2. Structure of AuMUA-AgTMA binary crystals. (**A**) Small-angle powder XRD spectrum of the crystals. Bragg reflections on planes specified by Miller indices shown are characteristic of a diamond-like structure. (Inset) Comparison between experimental (d^e) and theoretical (d^t) spacing between crystal planes with Miller indices [*hkl*]. Values of d^t were calculated based on the lattice constant a = 19.08 nm. The center-to-center distance between nanoparticles on the (100) face, calculated as $D = \sqrt{2}a/2$, is $D = 13.49 \pm 0.37$ nm; interparticle distance along body-diagonal axis calculated from XRD data is 8.27 ± 0.26 nm. (**B**) An SEM image of a $\{100\}_{SL}$ square face taken from a twinned-octahedron crystal (inset); estimated lattice constant a = 18.5 nm. (**C**) An SEM image of a $\{111\}_{SL}$ plane of a triangular face of an octahedron (inset) with estimated interparticle distance of 8.5 nm. (**D**) Scheme of an AB unit cell and the projections of $\{100\}_{SL}$, $\{110\}_{SL}$, $\{111\}_{SL}$ planes. NPs of one type are positioned in the nodes of a face-centered cubic lattice, whereas the others occupy half of the tetrahedral voids. The crystals are isostructural with sphalerite ZnS (SG 216) or, for crystals made of only one type of metal cores (compare Fig. 5B), with the diamond lattice (SG 227).

nature COMMUNICATIONS

ARTICLE

Received 30 Jul 2015 | Accepted 26 Oct 2015 | Published 2 Dec 2015

DOI: 10.1038/ncomms10052 OPEN

Structural diversity in binary superlattices self-assembled from polymer-grafted nanocrystals

Xingchen Ye[1], Chenhui Zhu[2], Peter Ercius[3], Shilpa N. Raja[4,5], Bo He[6], Matthew R. Jones[1], Matthew R. Hauwiller[1], Yi Liu[6], Ting Xu[4,5] & A. Paul Alivisatos[1,5,7]

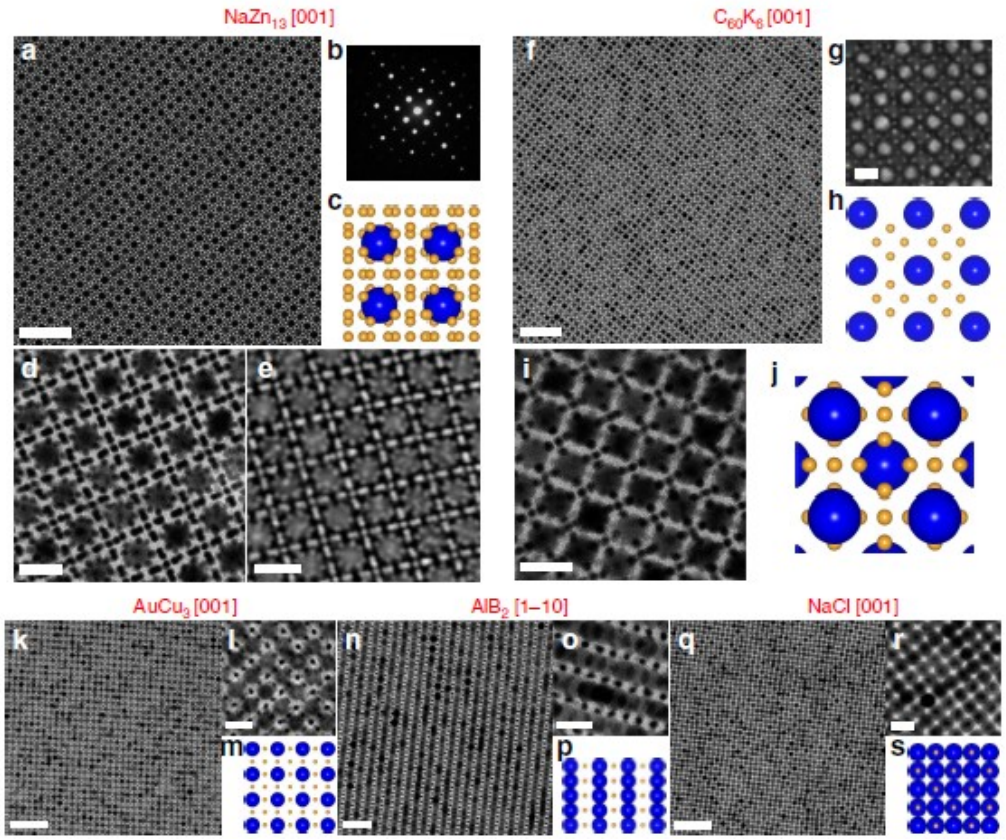

Figure 2 | Structural diversity in 3D BNSLs self-assembled from 3.8 nm (3.0 k) Au and 13.4 nm (5.3 k) Fe_3O_4 NCs. (**a**) Low-magnification TEM image and (**b**) corresponding SAED pattern, (**d**) high-magnification TEM image and (**e**) HAADF-STEM image of $NaZn_{13}$-type BNSLs. (**c**) Structural model of the [001] projection of $NaZn_{13}$-type BNSLs. (**f**) Low-magnification TEM image, (**i**) high-magnification TEM image and (**g**) SEM image of bcc-AB_6-type (isostructural with the $C_{60}K_6$ phase) BNSLs. (**h**,**j**) Structural models of the [001] projection (**j**) and the (001) surface (**h**) of bcc-AB_6-type BNSLs. (**k**,**n**,**q**) Low-magnification TEM images, (**l**,**o**,**r**) high-magnification TEM images and (**m**,**p**,**s**) structural models of $AuCu_3$-type (**k**–**m**), AlB_2-type (**n**–**p**) and NaCl-type (**q**–**s**) BNSLs. Scale bars, (**a**) 100 nm; (**d**) 20 nm; (**e**) 20 nm; (**f**) 100 nm; (**g**) 20 nm; (**i**) 20 nm; (**k**) 100 nm; (**l**) 20 nm; (**n**) 50 nm; (**o**) 20 nm; (**q**) 100 nm; (**r**) 20 nm.

Topotactic Interconversion of Nanoparticle Superlattices

13 SEPTEMBER 2013 VOL 341 SCIENCE www.sciencemag.org

Robert J. Macfarlane,[1,2] Matthew R. Jones,[2,3] Byeongdu Lee,[4] Evelyn Auyeung,[2,3] Chad A. Mirkin[1,2,3]*

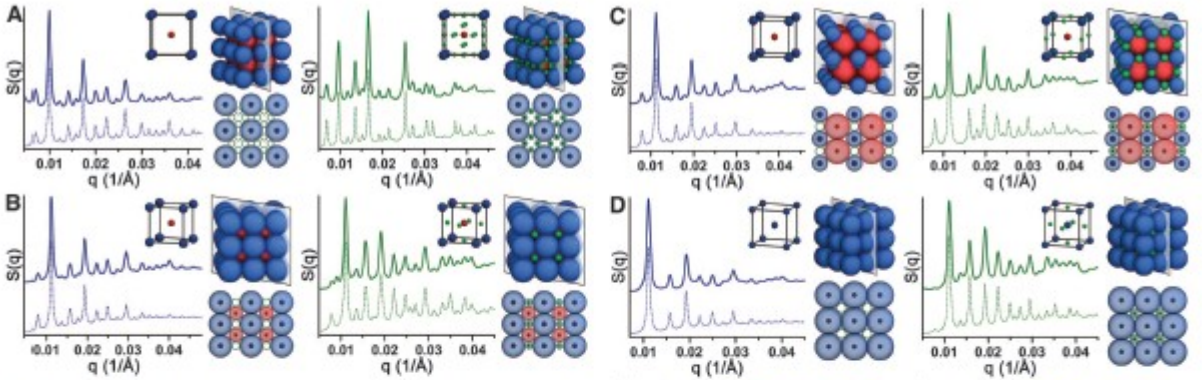

Fig. 2. SAXS data for binary parent and ternary daughter SLs. Experimental SAXS data (solid lines) are compared against theoretical predictions (dashed lines) for parent (blue) and daughter (green) SLs. Each corresponding SL is drawn to scale to the right of its SAXS data, where the top left inset shows the positions and relative sizes of the AuNPs alone and the top right inset shows the relative sizes of the full PAE hydrodynamic diameters. The bottom inset shows the 2D plane represented in the top right inset, demonstrating the AuNP positions and relative hydrodynamic diameters of the particles within that plane. The 2D planes of the parent SLs also show the pockets into which daughter NPs are inserted (dashed green outlines). The parent and daughter SLs are isostructural with (**A**) CsCl and ABC_{12}-type, (**B**) CsCl and face-perovskite, (**C**) CsCl and edge-perovskite, (**D**) bcc and A_2B_3-type, and (**E**) AlB_2- and AB_4-type geometries.

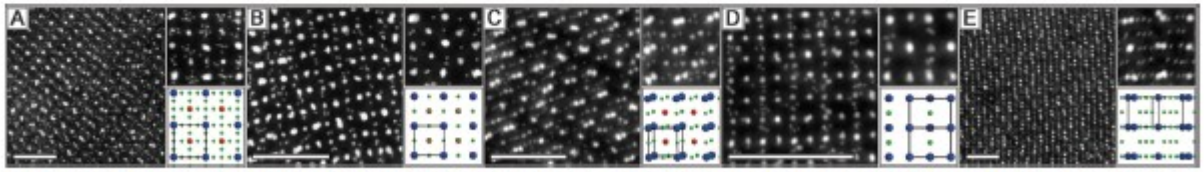

Fig. 3. TEM data for ternary NP SLs. DNA-linked NP SLs were embedded in silica to preserve their structure, then embedded in a commercially available resin and microtomed. TEM images of the microtomed sections show the incorporation of the daughter NPs into the parent SLs, in a lower magnification image (larger image, left), and a higher magnification image (right, top) that shows the SLs viewed along a specific orientation. An image of a modeled SL is provided for comparison (right, bottom) to demonstrate the angle at which the lattices are viewed in the higher magnification images. TEM images are for SLs isostructural with (**A**) ABC_{12}-type, (**B**) face-perovskite, (**C**) edge-perovskite, (**D**) A_2B_3-type, and (**E**) AB_4-type geometries. Scale bars, 200 nm.

Vol 439|5 January 2006|doi:10.1038/nature04414 nature

LETTERS

Structural diversity in binary nanoparticle superlattices

Elena V. Shevchenko[1,2]*†, Dmitri V. Talapin[1]*†, Nicholas A. Kotov[3], Stephen O'Brien[2] & Christopher B. Murray[1]

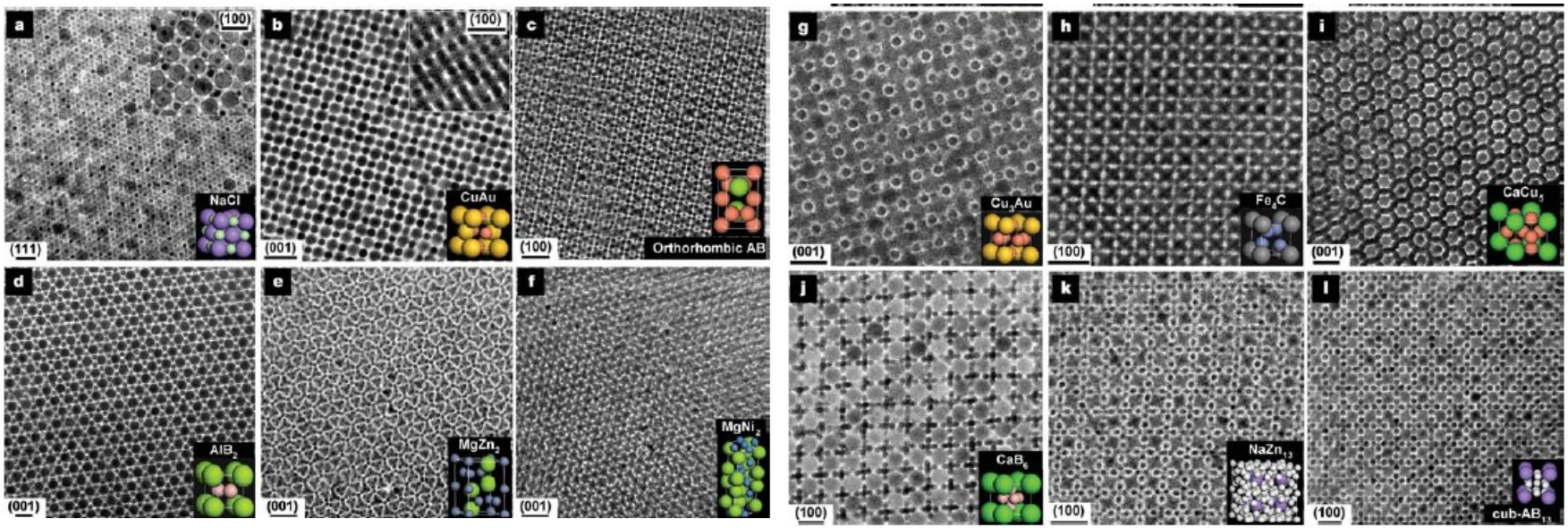

Figure 1 | TEM images of the characteristic projections of the binary superlattices, self-assembled from different nanoparticles, and modelled unit cells of the corresponding three-dimensional structures. The superlattices are assembled from **a**, 13.4 nm γ-Fe_2O_3 and 5.0 nm Au; **b**, 7.6 nm PbSe and 5.0 nm Au; **c**, 6.2 nm PbSe and 3.0 nm Pd; **d**, 6.7 nm PbS and 3.0 nm Pd; **e**, 6.2 nm PbSe and 3.0 nm Pd; **f**, 5.8 nm PbSe and 3.0 nm Pd; **g**, 7.2 nm PbSe and 4.2 nm Ag; **h**, 6.2 nm PbSe and 3.0 nm Pd; **i**, 7.2 nm PbSe and 5.0 nm Au; **j**, 5.8 nm PbSe and 3.0 nm Pd; **k**, 7.2 nm PbSe and 4.2 nm Ag; and **l**, 6.2 nm PbSe and 3.0 nm Pd nanoparticles. Scale bars: **a**–**c**, **e**, **f**, **i**–**l**, 20 nm; **d**, **g**, **h**, 10 nm. The lattice projection is labelled in each panel above the scale bar. The modelled projections of the binary superlattices are shown in Supplementary Fig. 4.

3D ordered binary SLs (BNSLs) of Au and Fe_2O_3 NPs

Control of crystalline structure with different effective size ratio (Fe_2O_3-Au)

TEM

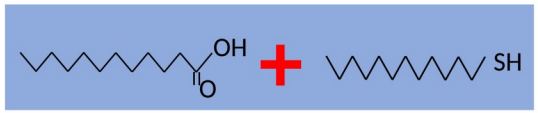

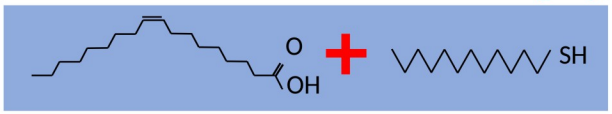

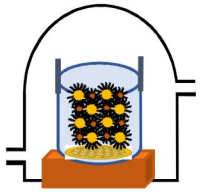

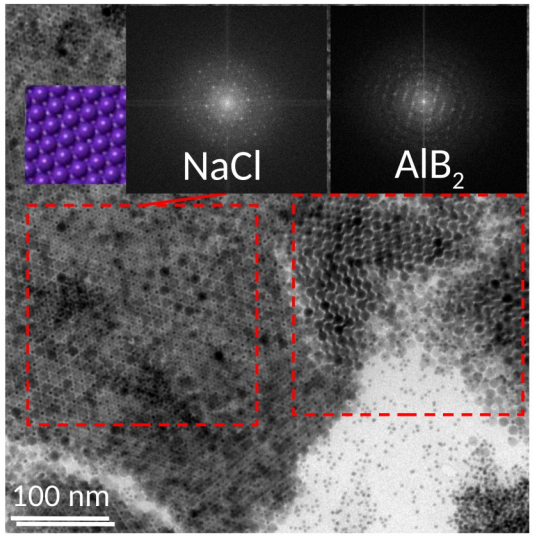

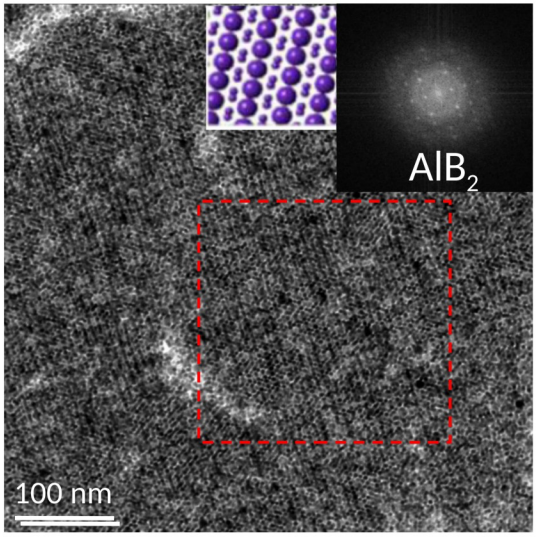

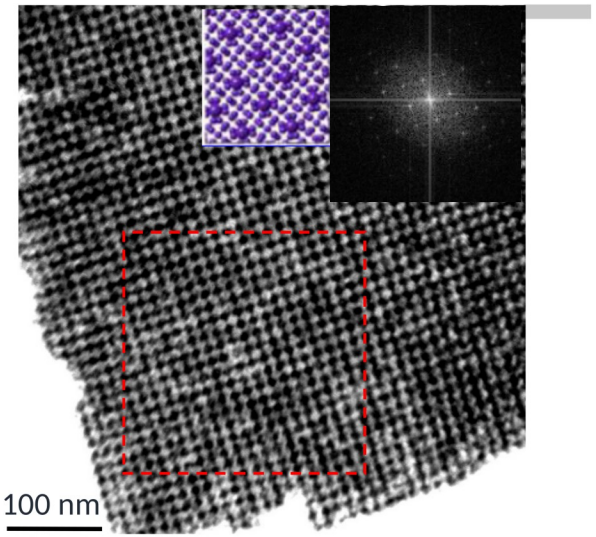

NP_1	NP_2	Concentration (Ref: $5x10^{-7}$ M)	Effective size ratio (NP_2/NP_1)	Structure
Fe_2O_3 (12.4nm, C_{12})	Au(4.6nm, C_{12})	1:4	0.46	$NaCl+AlB_2$
Fe_2O_3 (11.4nm, C_{18})			0.49	AlB_2
Fe_2O_3 (7.9nm, C_{18})			0.66	$NaZn_{13}$

➢ **Effective size ratio and the nature of the ligands affect the crystalline structure.**

PhD Thesis of Suyeon Lee, laboratoire MONARIS, Paris France

Thanks to Alexa Courty

3D ordered BNSLs of Au and Fe_2O_3 NPs

SEM

NaCl structure

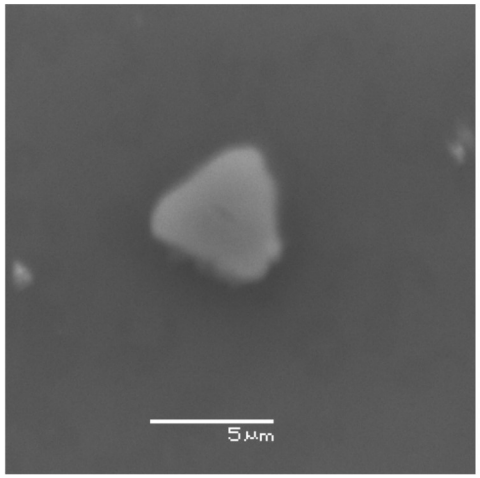

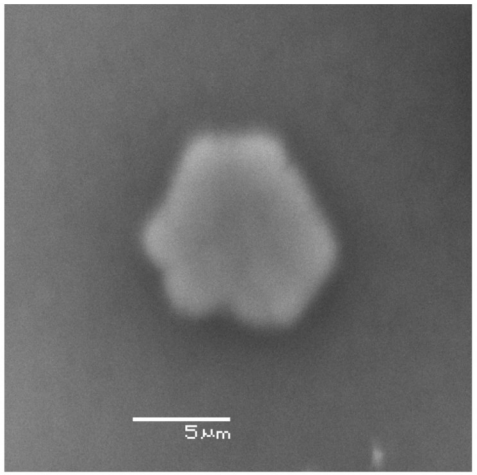

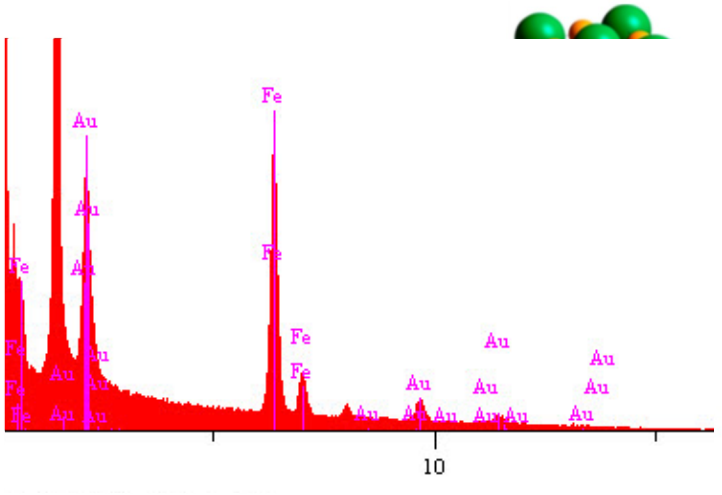

EDS : Fe 80%, Au 20%

$NaZn_{13}$ structure

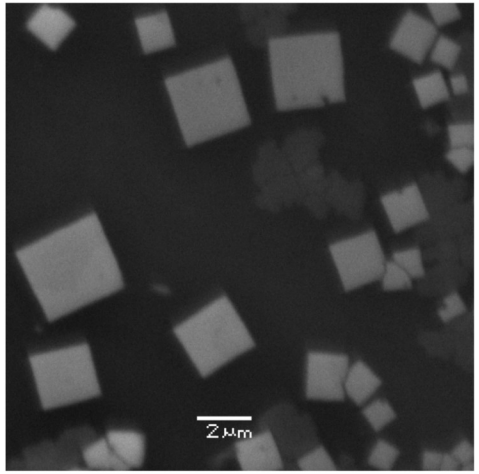

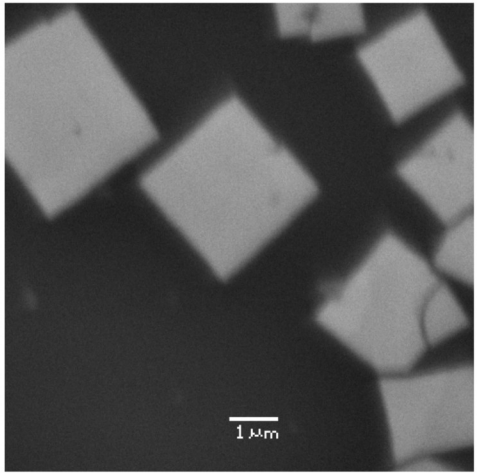

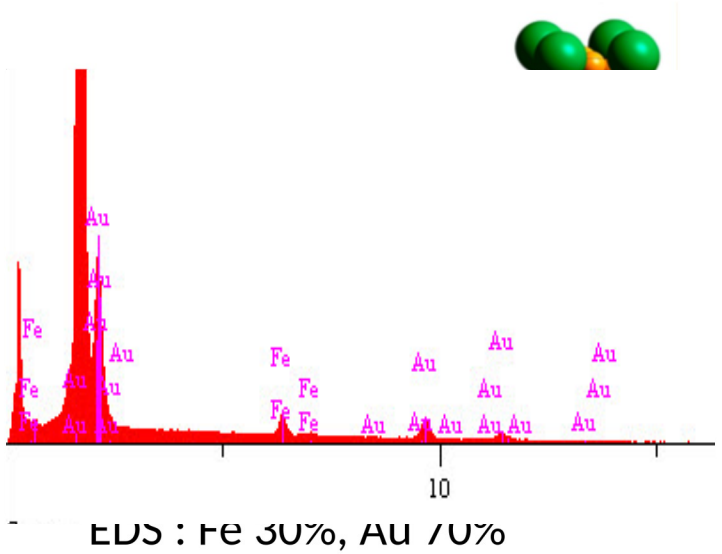

EDS : Fe 30%, Au 70%

PhD Thesis of Suyeon Lee, laboratoire MONARIS, Paris France

Thanks to Alexa Courty

3D ordered BNSLs of Au and Fe_2O_3 NPs

HR-SEM images on $NaZn_{13}$ BNLs

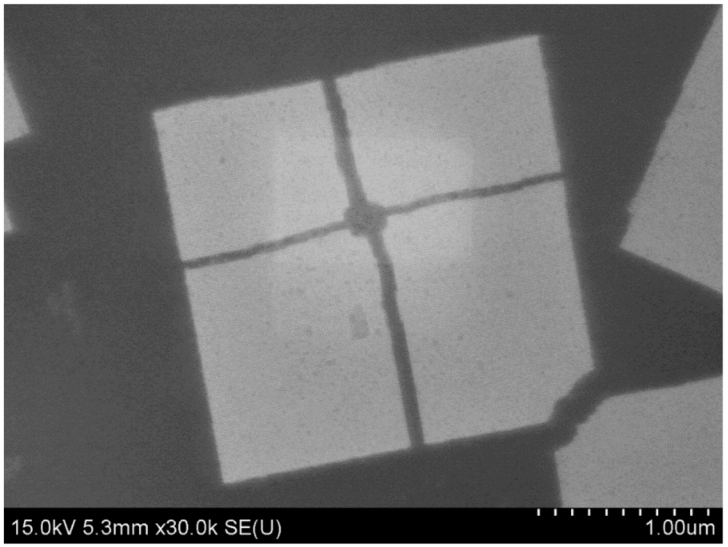

zoom

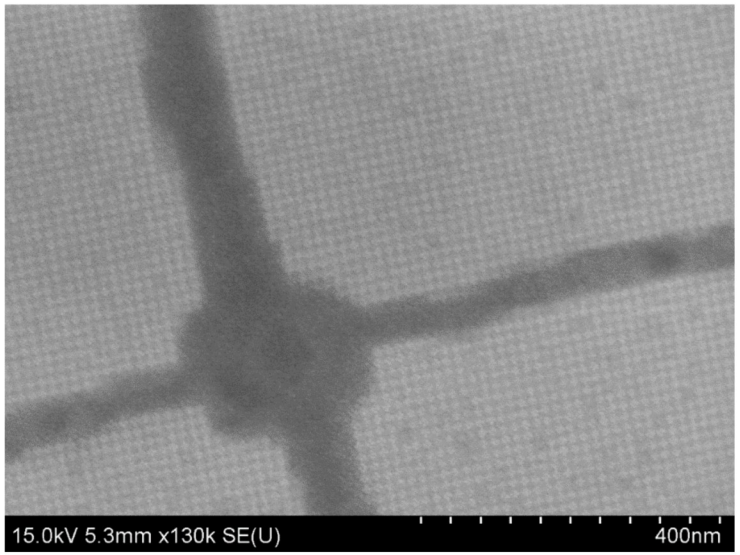

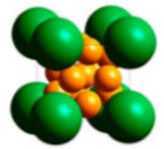

zoom

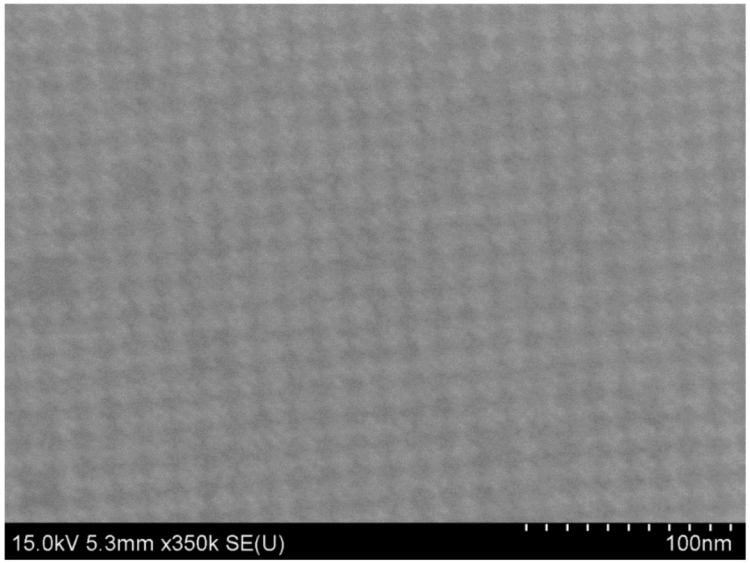

zoom

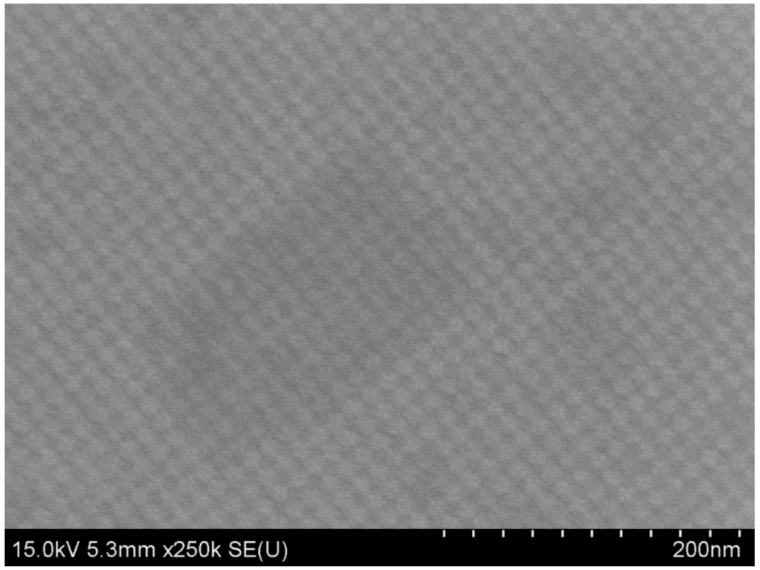

PhD Thesis of Suyeon Lee, laboratoire MONARIS, Paris France

Thanks to Alexa Courty

JACS
JOURNAL OF THE AMERICAN CHEMICAL SOCIETY

Ligand Exchange Governs the Crystal Structures in Binary Nanocrystal Superlattices

Jingjing Wei,[†,‡] Nicolas Schaeffer,[†,‡] and Marie-Paule Pileni*[,†,‡,§]

[†]Sorbonne Universités, UPMC Université Paris 06, UMR 8233, MONARIS, F-75005 Paris, France
[‡]CNRS, UMR 8233, MONARIS, F-75005 Paris, France
[§]CEA/IRAMIS, CEA Saclay, 91191 Gif-sur-Yvette, France

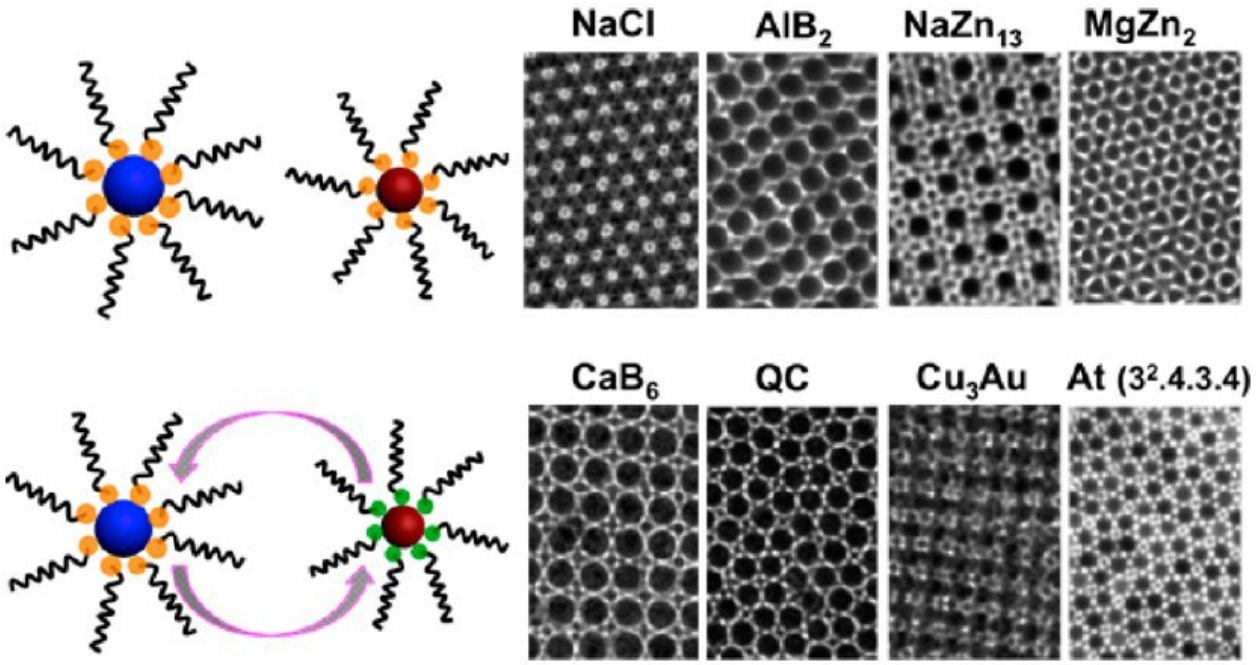

DOI: 10.1021/jacs.5b09959
J. Am. Chem. Soc. 2015, 137, 14773−14784

nature Vol 461|15 October 2009|doi:10.1038/nature08439

LETTERS

Quasicrystalline order in self-assembled binary nanoparticle superlattices

Dmitri V. Talapin[1,2]*, Elena V. Shevchenko[2]*, Maryna I. Bodnarchuk[1], Xingchen Ye[3], Jun Chen[4] & Christopher B. Murray[3,4]

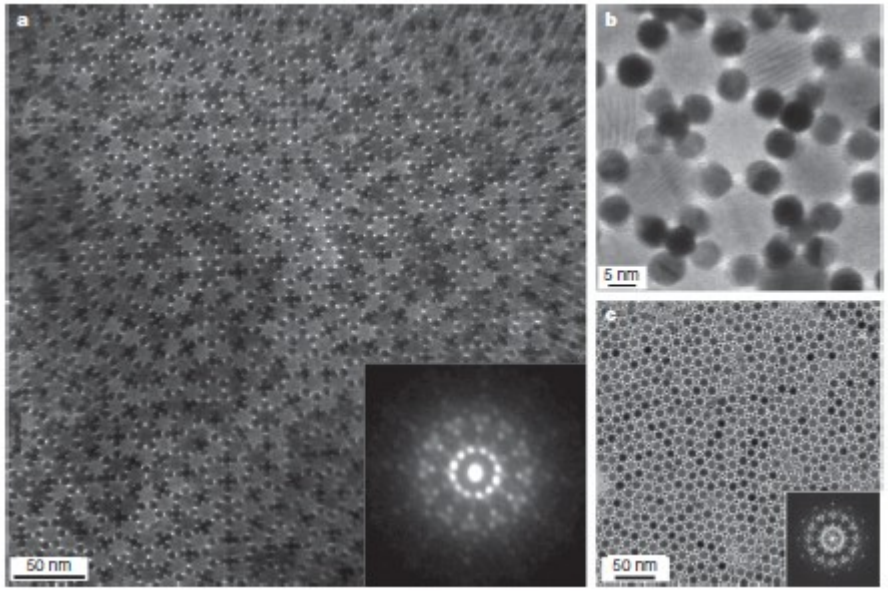

Figure 2 | Dodecagonal quasicrystals self-assembled from spherical nanoparticles. **a**, TEM image of a quasicrystalline superlattice self-assembled from 13.4-nm Fe_2O_3 and 5-nm Au nanocrystals. Inset, selected-area electron diffraction pattern with non-crystallographic 12-fold rotational symmetry measured from a ~6-μm^2 domain. **b**, Magnified view of a dodecagonal nanoparticle quasicrystal. **c**, Dodecagonal quasicrystalline superlattice self-assembled from 9-nm PbS and 3-nm Pd nanocrystals. Inset, fast-Fourier-transform pattern of the quasicrystalline superlattice.

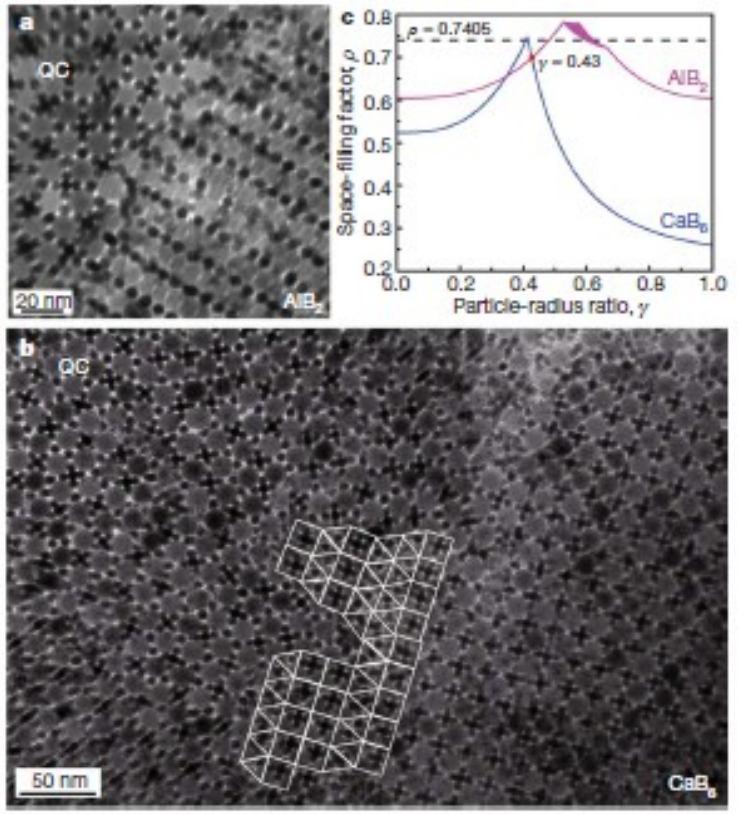

Figure 3 | Structure of the interface between quasicrystalline and crystalline phases. **a**, Interface between the DDQC phase and the AlB_2-type binary superlattice self-assembled from 13.4-nm Fe_2O_3 and 5-nm Au nanocrystals. QC, quasicrystal. **b**, Transition from the DDQC phase to the CaB_6-type binary superlattice of 12.6-nm Fe_3O_4 and 4.7-nm Au nanocrystals is facilitated by the presence of a 'wetting layer' of $(3^3.4^2)$ Archimedean tiling. **c**, Space-filling factors calculated for the AlB_2 and CaB_6 structures. The dotted line corresponds to the single-component close-packed structure with the space-filling factor $\rho = 0.7405$. The filled-in section in the AlB_2 line corresponds to different arrangements of densely packed spheres.

nature Vol 466|22 July 2010|doi:10.1038/nature09

LETTERS

Binary nanocrystal superlattice membranes self-assembled at the liquid–air interface

Angang Dong[1], Jun Chen[2], Patrick M. Vora[3], James M. Kikkawa[3] & Christopher B. Murray[1,2]

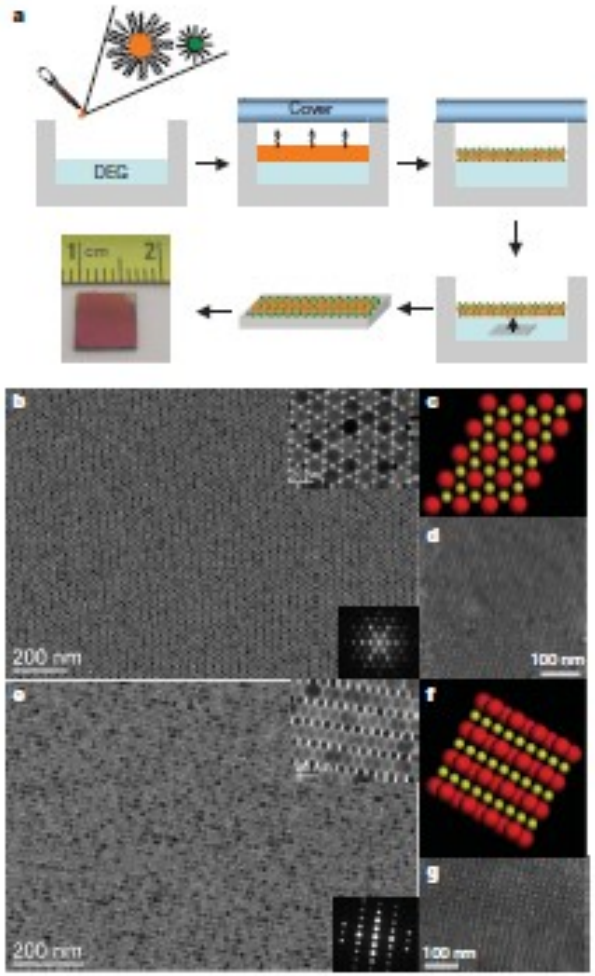

Figure 1 | Large-scale BNSL membranes self-assembled at the liquid–air interface. **a**, Schematic of the BNSL membrane growth and transfer processes. The photograph shows a typical BNSL membrane transferred to a SiO_2–Si wafer. Mechanical damage from tweezers in the membrane's upper right corner (photo) helps visualize the scale. **b**–**g**, AlB_2-type BNSL membranes self-assembled from 15-nm Fe_3O_4 and 6-nm FePt nanocrystals. **b**, TEM image of the (001) lattice projection (upper inset, magnified view; lower inset, small-angle electron diffraction pattern). **c**, **d**, Crystallographic model (**c**) and high-resolution scanning electron microscopy (HRSEM; **d**) image of the (001) projection. **e**, TEM image of the (100) lattice projection (upper inset, magnified view; lower inset, small-angle electron diffraction pattern). **f**, **g**, Crystallographic model (**f**) and HRSEM image of the (100) projection (**g**).

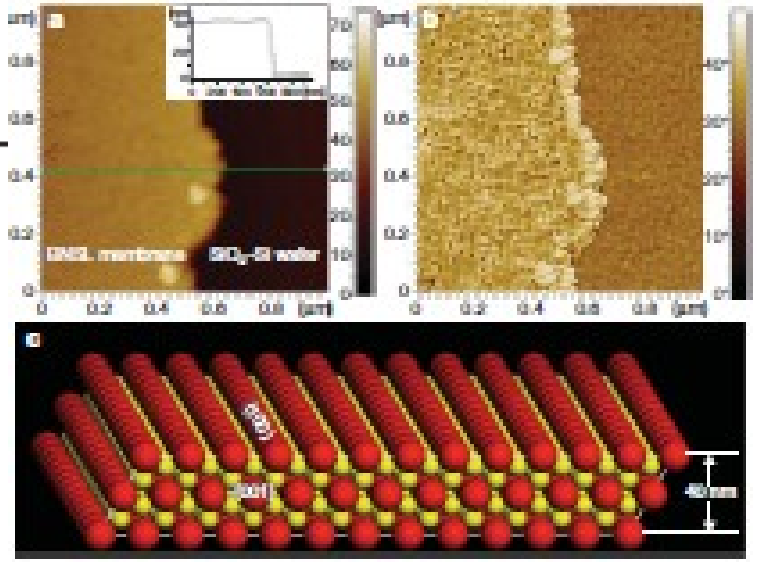

Figure 2 | BNSL membrane one unit cell thick. **a**, AFM height image (scan size, 1 μm × 1 μm) of an AlB_2-type BNSL membrane consisting of 15-nm Fe_3O_4 and 6-nm FePt nanocrystals. Inset, height analysis of the profile indicated in the AFM image. **b**, AFM phase image of the same membrane, showing a (100) projection in plane view. **c**, Side view of a crystallographic model of the membrane, showing that the membrane is one unit cell thick.

LETTERS
PUBLISHED ONLINE: 26 SEPTEMBER 2016 | DOI: 10.1038/NMAT4759
nature materials

Quasicrystalline nanocrystal superlattice with partial matching rules

Xingchen Ye[1†], Jun Chen[1,2†], M. Eric Irrgang[3,4†], Michael Engel[4,5†], Angang Dong[6], Sharon C. Glotzer[3,4,5*] and Christopher B. Murray[1,2*]

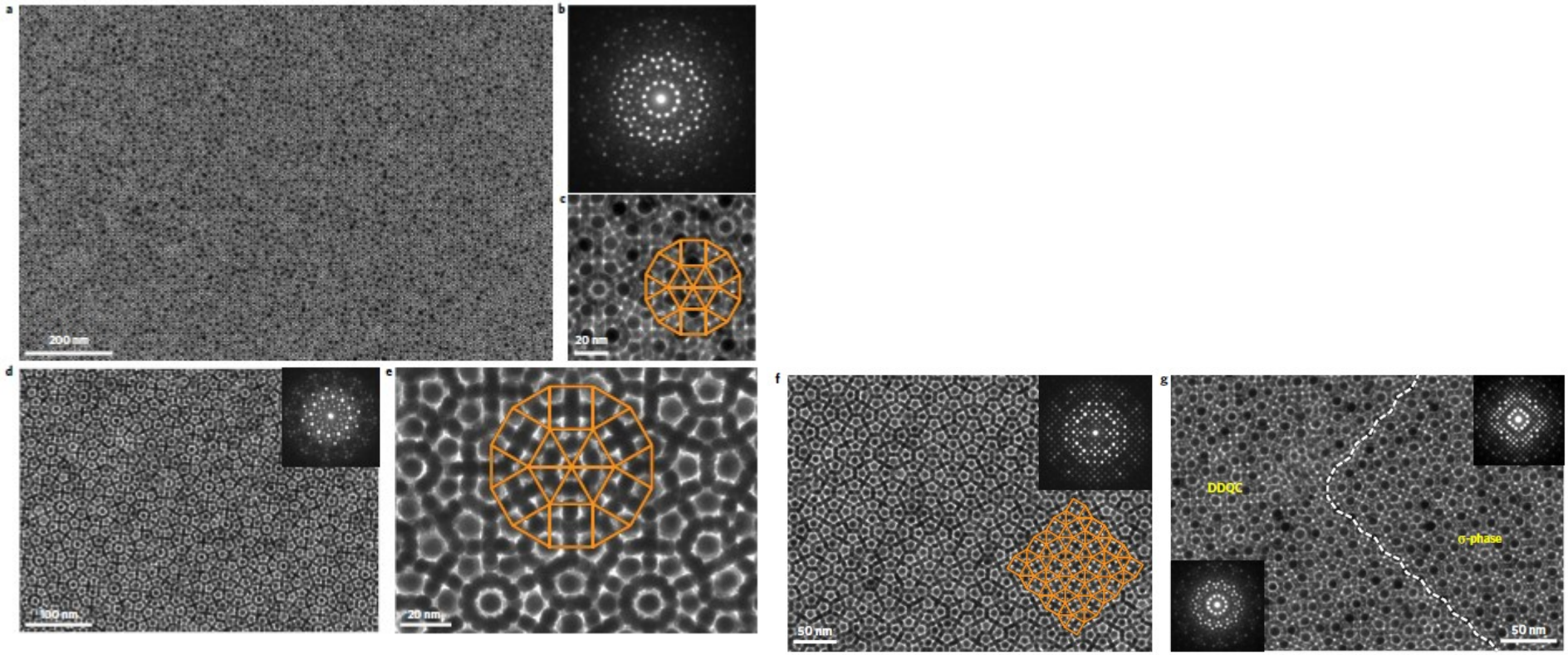

Figure 1 | Self-assembled binary NC superlattices with quasiperiodic and periodic order. a–c, Low-magnification TEM image (**a**), SAED pattern (**b**) and high-magnification TEM image (**c**) of a dodecagonal quasicrystal self-assembled from 6.8 nm $CoFe_2O_4$ and 12.0 nm Fe_3O_4 NCs. **d**,**e**, Low-magnification TEM image and SAED pattern (inset) (**d**) and high-magnification TEM image (**e**) of the quasicrystal self-assembled from 6.2 nm FePt and 11.5 nm Fe_3O_4 NCs. **f**, TEM image and SAED pattern (inset) of the competing periodic σ-phase in a FePt–$CoFe_2O_4$ superlattice. The $3^2.4.3.4$ tiling of the σ-phase is shown as an overlay. **g**, TEM image and SAED patterns (insets) show the coexistence of the quasicrystal and the σ-phase in a $CoFe_2O_4$–Fe_3O_4 superlattice.

Granular segregation

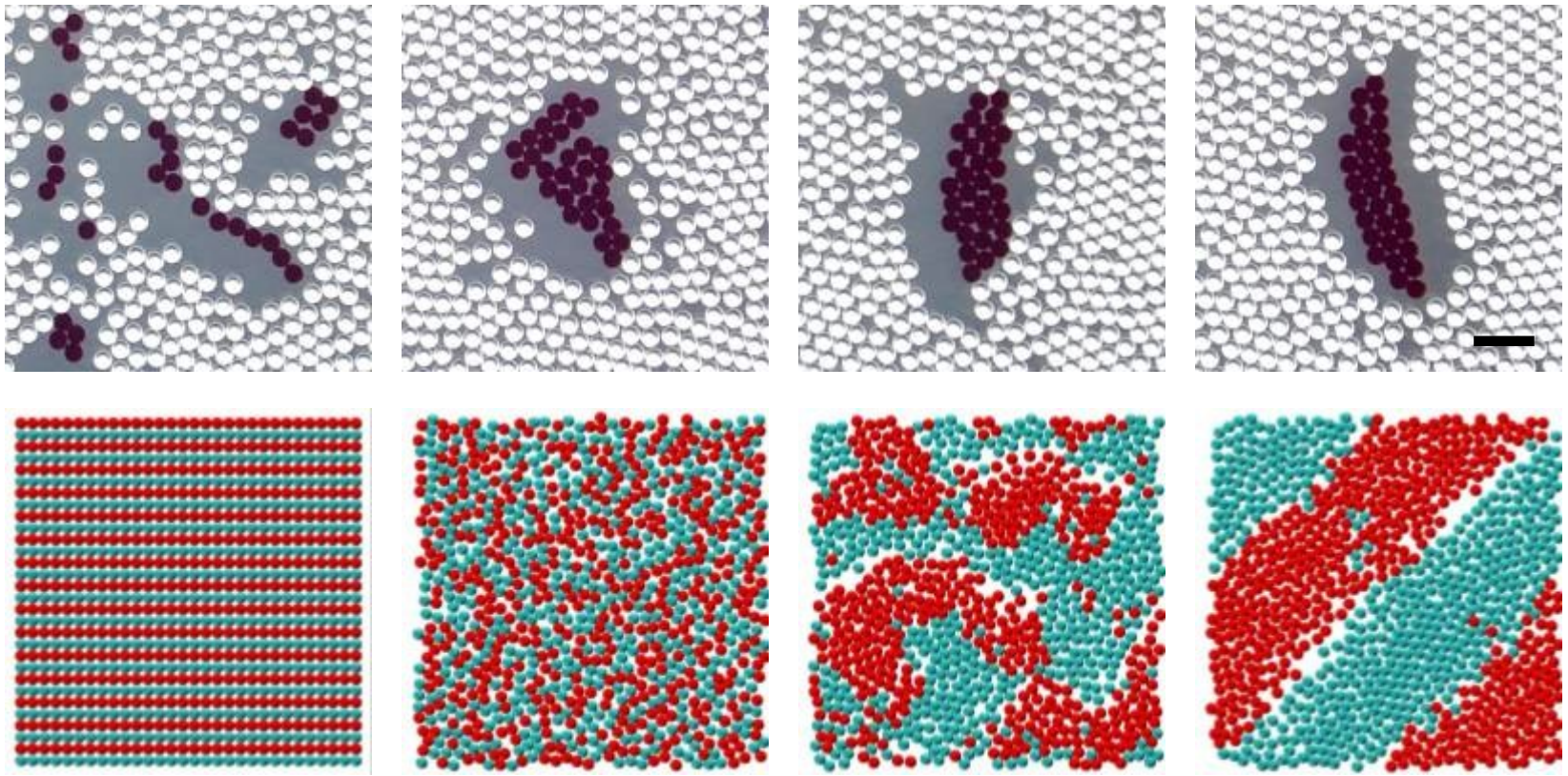

With Michael Grünwald, Phillip Geissler

Granular segregation

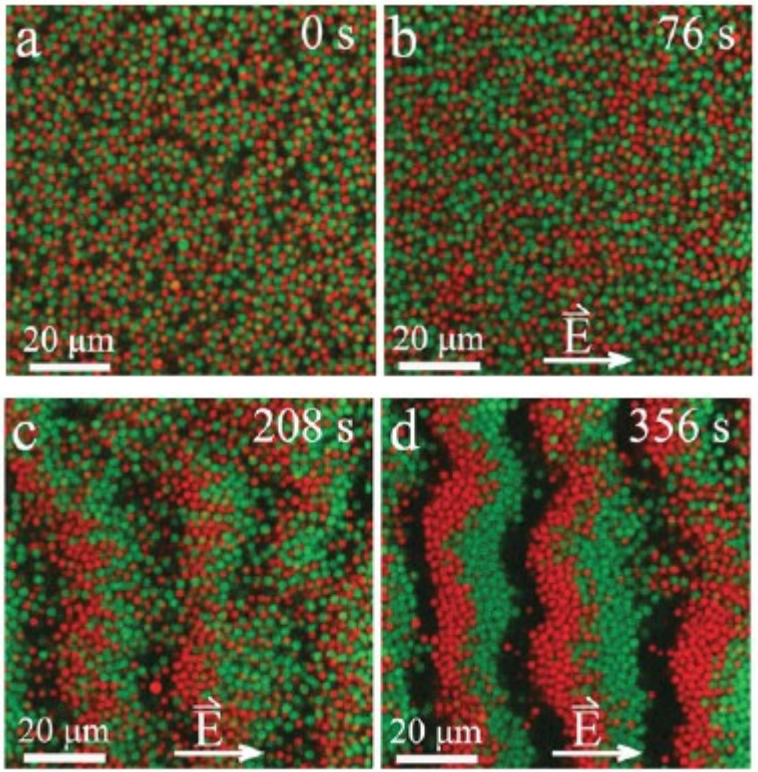

FIG. 1 (color). Band formation of oppositely charged colloids with a diameter of ca. 2.5 μm in an ac electric field with strength $|E| = 17.5$ V/mm, and frequency $f = 0.02$ Hz. (a) No field is applied and the mixture is isotropic, (b) locally bands start to form after 76 s, (c) the bands become more pronounced, and (d) the bands are clearly delineated.

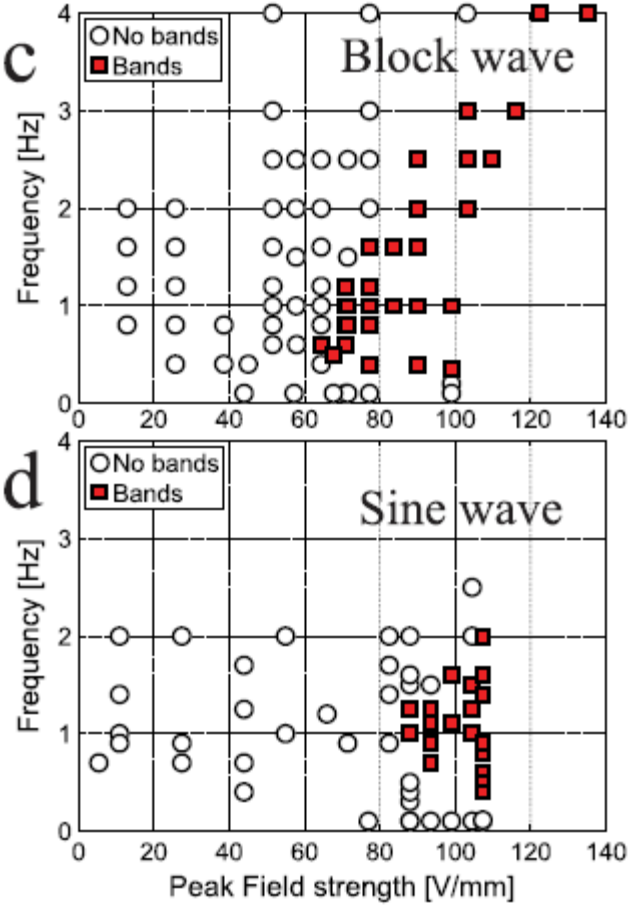

T. Vissers, A. van Blaaderen and A. Imhof, *Phys. Rev. Lett.*, 2011, **106**, 228303

Nanoobjects

Self-assembly of nanoobjects

Binary assemblies

Molecule oriented supraparticular chemistry

CONTEXT

VERY OFTEN

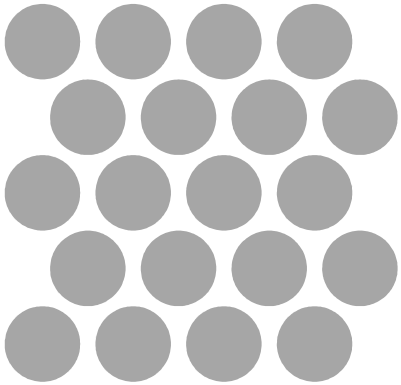

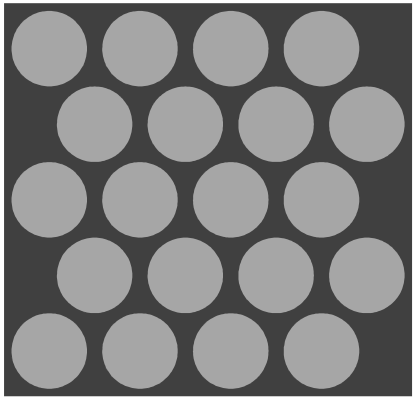

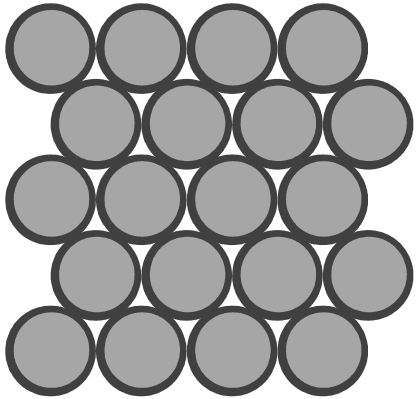

CONTEXT

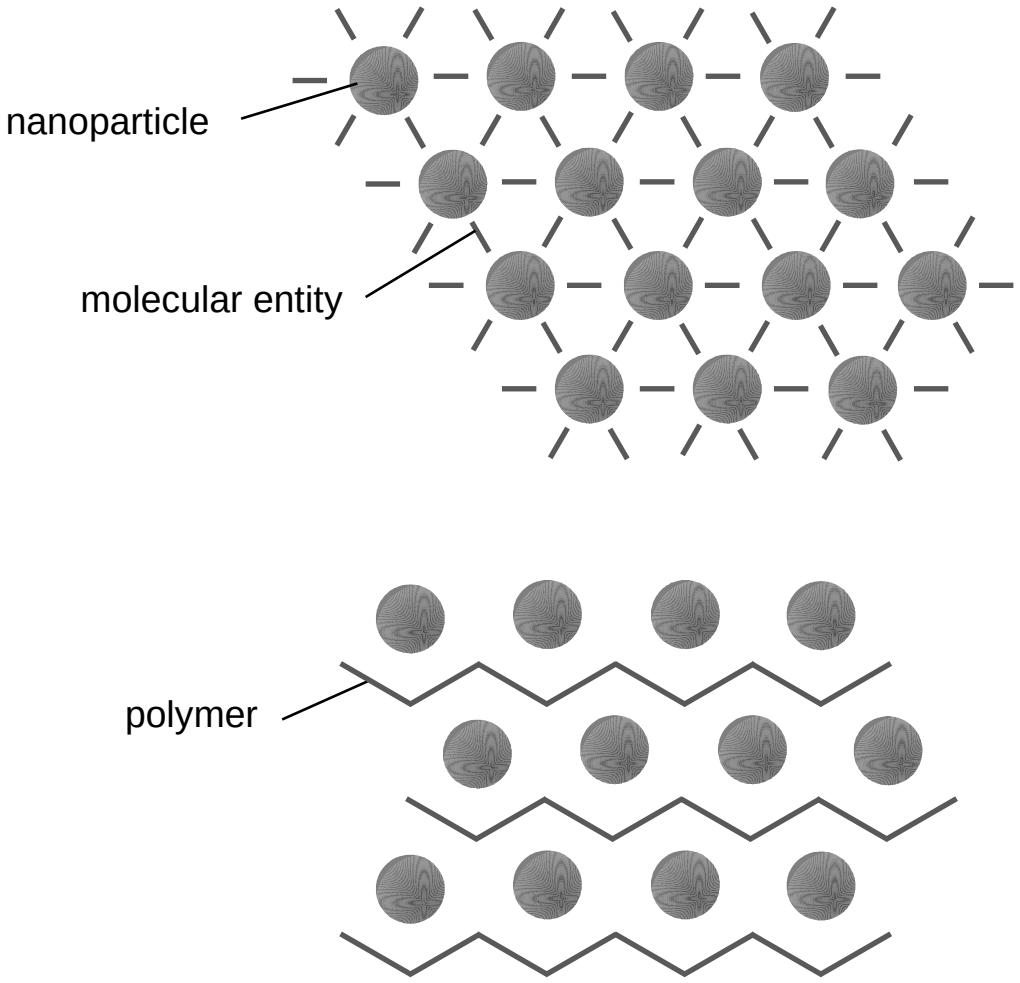

Structural and/or functional synergies
Energy transfer / interactions

CONTEXT

RESPONSIVE LIGANDS

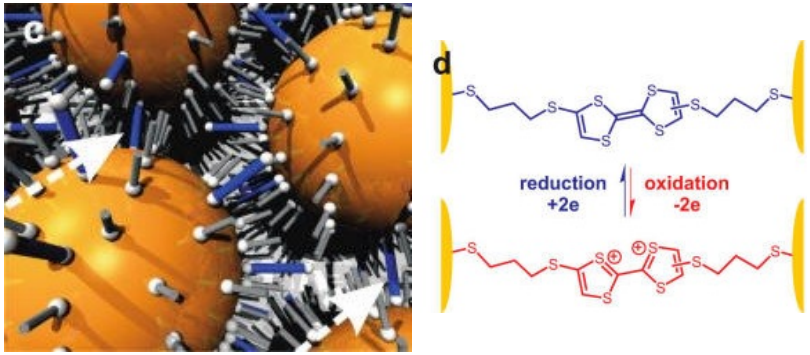

Calame, et al. 2010

ASYMETRIC FUNCTIONALIZATION

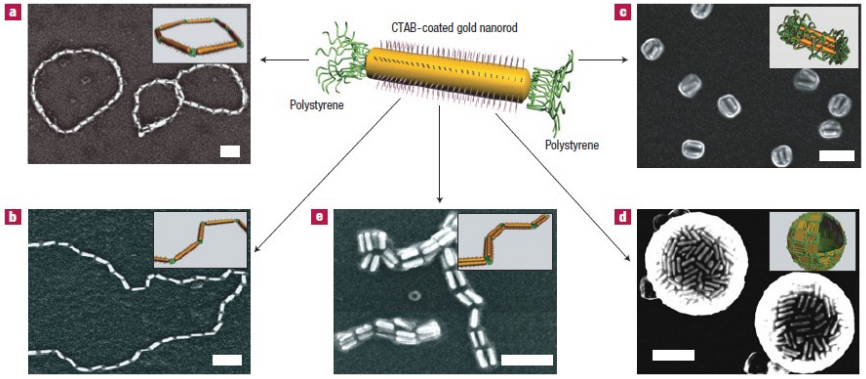

Kumacheva, et al. 2007

DNA

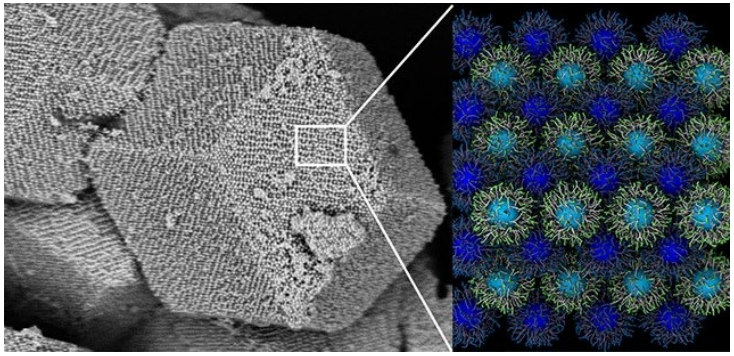

Mirkin, et al. 2014

DIBLOCK COPOLYMER

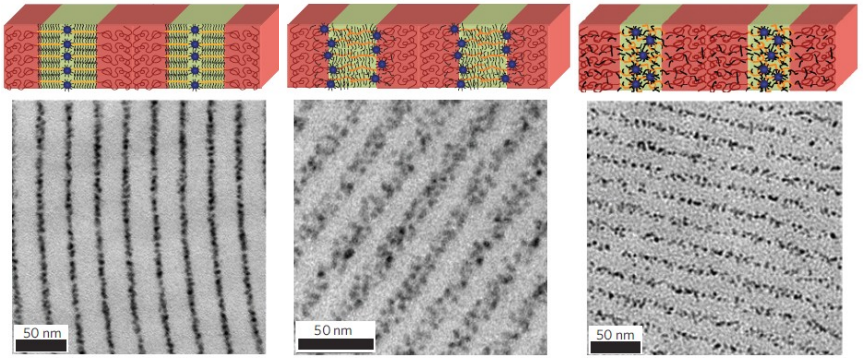

Xu, et al. 2009